Sterile neutrinos with non-standard interactions in β- and $0\nu\beta\beta$-decay experiments

W. Dekens,[a] **J. de Vries**[b,c] **and T. Tong**[b,d]

[a]*Department of Physics, University of California at San Diego,*
La Jolla, CA 92093, U.S.A.

[b]*Institute for Theoretical Physics Amsterdam and Delta Institute for Theoretical Physics,*
University of Amsterdam,
Science Park 904, 1098 XH Amsterdam, The Netherlands

[c]*Nikhef, Theory Group,*
Science Park 105, 1098 XG, Amsterdam, The Netherlands

[d]*Institute for Fundamental Science and Department of Physics, University of Oregon,*
Eugene, OR 97403, U.S.A.

E-mail: wgdekens@gmail.com, j.devries4@uva.nl, tomtong2015@gmail.com

ABSTRACT: Charged currents are probed in low-energy precision β-decay experiments and at high-energy colliders, both of which aim to measure or constrain signals of beyond-the-Standard-Model physics. In light of future β-decay and LHC measurements that will further explore these non-standard interactions, we investigate what neutrinoless double-β decay ($0\nu\beta\beta$) experiments can tell us if a nonzero signal were to be found. Using a recently developed effective-field-theory framework, we consider the effects that interactions with right-handed neutrinos have on $0\nu\beta\beta$ and discuss the range of neutrino masses that current and future $0\nu\beta\beta$ measurements can probe, assuming neutrinos are Majorana particles. For non-standard interactions at the level suggested by recently observed hints in β decays, we show that next-generation $0\nu\beta\beta$ experiments can determine the Dirac or Majorana nature of neutrinos, for sterile neutrino masses larger than $\mathcal{O}(10)\,\mathrm{eV}$.

KEYWORDS: Beyond Standard Model, Effective Field Theories, Neutrino Physics

Contents

1 Introduction

Investigations of β-decay processes have played an important role in the development of the Standard Model (SM) of particle physics. In the modern era, precision analyses of pion, neutron, and nuclear β-decay are used to extract precise values of SM parameters (in particular $V_{ud}G_F$) and to probe beyond-the-Standard-Model (BSM) physics. At the relatively low energies associated with β-decay experiments, which involve Q-values around an MeV, BSM physics can be described using effective-field-theory (EFT) techniques as was already proposed by Lee and Yang [1], for recent reviews see e.g. refs. [2–7]. Within this framework the $V - A$ structure of the SM charged weak interaction is described by a dimension-six operator, while deviations are captured by additional higher-dimensional operators which are suppressed by powers of v/Λ, where $v \simeq 246\,\mathrm{GeV}$ is the electroweak scale and Λ the scale of new physics. At the leading dimension-six level, the SM current is then augmented by ten effective interactions each of which comes with an, in principle complex, Wilson coefficient that scales as v^2/Λ^2.

These charged-current interactions can be investigated both at high energies, e.g. in $pp \to e\nu$ at the LHC, as well as in low-energy precision measurements. Focussing on probes in the latter category, Falkowski, González-Alonso, and Naviliat-Cuncic recently performed a state-of-the-art analysis of neutron and nuclear β-decay data [8] (we will refer to this work by FGN). In addition to neutron decay and superallowed $0^+ \to 0^+$ transitions, FGN included data from mirror $1/2^+ \to 1/2^+$ decays. The authors then performed a simultaneous fit including all leading-order dimension-six Wilson coefficients (considering only the real parts), while taking into account theory uncertainties by marginalizing over nuisance parameters related to radiative corrections and nuclear matrix elements (NMEs). Armed with this framework, FGN then analyzed all relevant data in several scenarios. Assuming only SM interactions FGN obtained accurate values for $V_{ud} = 0.97370(25)$ and $g_A = 1.27276(45)$, illustrating that β-decay experiments can be used to extract precise determinations of fundamental SM parameters and hadronic matrix elements. Adding non-standard interactions involving only left-handed neutrinos to the global fit gives an impressive confirmation of the SM: non-standard scalar and tensor interactions are constrained at the per-mille level, corresponding to scales of BSM physics of several TeV (note that pseudoscalar interactions give suppressed contributions and were not considered). Assuming the BSM scale is well above the electroweak scale, LHC measurements can be used to derive similar, complementary, constraints [2, 3].

This picture changes somewhat once non-standard interactions involving right-handed neutrinos are included as well. In this case, the global fit constrains vector, axial-vector, and scalar couplings to right-handed neutrinos at the few percent level, but prefers a nonzero right-handed tensor coupling at the 10% level (about 3.2σ away from the SM point). This discrepancy is driven by a single recent measurement of the "little-a" coefficient in neutron decay [9] and is not significant enough to warrant too much excitement. In particular it is unclear whether one can construct a viable BSM scenario, given the current LHC constraints from $pp \to e\nu$ [2, 3]. Nevertheless, in light of the FGN result, the recent hints for BSM effects in CKM unitarity tests [10–13], and more generally in context of ongoing and future β-decay experiments and collider measurements, it is interesting to ask what a signal of BSM charged-currents would imply for other complementary experiments. For instance, refs. [2, 3] demonstrated a strong complementarity between β-decay and LHC observables.

Here we focus on couplings to right-handed neutrinos and the connection to probes of lepton number violation (LNV). The presence of right-handed neutrinos in nature would imply the existence of fields that are neutral under the full SM gauge group.[1] As a result, nothing forbids the existence of a Majorana mass for fields like this unless additional symmetries are invoked. Such a mass term would imply that the mass eigenstates of neutrinos are Majorana and the violation of Lepton Number (L) by two units. So, if β-decay or collider experiments uncover evidence for right-handed neutrino interactions, a reasonable follow-up question would be: in which scenarios can we expect to find correlated signals in

---

[1]They do not have be singlets under BSM gauge groups. For example, in left-right symmetric models [14–16] the right-handed neutrinos are charged under $SU(2)_R$ and couple to right-handed gauge bosons. At low energies, the right-handed neutrinos are sterile with respect to the SM gauge group, but interact through higher-dimension couplings that arise from integrating out the heavy BSM fields.

experimental probes of LNV? Here, we investigate this question in the context of searches for neutrinoless double beta decay ($0\nu\beta\beta$), the process where two neutrons in a nucleus transform into two protons with the emission of two electrons but zero (anti-)neutrinos.

To compare constraints from β- and $0\nu\beta\beta$-decay experiments on couplings to right-handed neutrinos we need to consider the mass scale of right-handed neutrinos. β decays are insensitive to neutrino masses whenever the neutrinos are light, $m_i \ll Q$, while a $0\nu\beta\beta$ signal is proportional to the Majorana masses of the neutrinos. We therefore focus on right-handed neutrinos with masses well below the MeV scale that can be considered approximately massless for β decay experiments (as well as at colliders). Additional constraints on sterile neutrinos could in principle come from cosmological and astrophysical probes [17, 18] such as big bang nucleosynthesis [19, 20] considerations or the cosmic microwave background [21]. Such constraints however depend on the thermal history of the universe and can be avoided in specific scenarios [22].

In what follows, we calculate the expected $0\nu\beta\beta$ decay rates of various isotopes as a function of the non-standard couplings and the right-handed neutrino mass. Barring significant cancelations between the contributions from the 'standard mechanism' and those from sterile neutrinos, we then discuss the range of neutrino masses for which a β-decay or collider signal could imply a measurable signal in $0\nu\beta\beta$. We start by setting up the EFT framework in section 2 and briefly describe the FGN analysis in section 3.1. The $0\nu\beta\beta$ decay rates in the presence of light right-handed neutrinos with non-standard interactions are discussed in section 3.2. We present our analysis of EFT couplings in section 4 and consider a specific BSM model involving leptoquarks in section 5. We conclude in section 6. Appendices are devoted to the matching relations with the neutrino-extended Standard Model Effective Field Theory and the calculation of $0\nu\beta\beta$ decay rates.

2 The Lagrangian in the Standard Model Effective Field Theory

In this work, we focus on interactions that give rise to β decays, especially those that involve right-handed neutrinos. We therefore consider an effective field theory that consists of the SM supplemented by an SM gauge singlet, ν_R, and include higher-dimensional operators up to dimension six. The Lagrangian of the resulting EFT, called the neutrino-extended Standard Model EFT (νSMEFT) can then be written as

$$\mathcal{L} = \mathcal{L}_{SM} + \bar{\nu}_R \, i\slashed{\partial} \nu_R - \left[\frac{1}{2} \bar{\nu}_R^c \, \bar{M}_R \nu_R + \bar{L} \tilde{H} Y_\nu \nu_R + \text{h.c.} \right]$$
$$+ \mathcal{L}_{\nu_L}^{(\bar{5})} + \mathcal{L}_{\nu_R}^{(\bar{5})} + \mathcal{L}_{\nu_L}^{(\bar{6})} + \mathcal{L}_{\nu_R}^{(\bar{6})}, \tag{2.1}$$

where we used $\Psi^c = C\bar{\Psi}^T$ for a field Ψ in terms of the charge conjugation matrix $C = -C^{-1} = -C^T = -C^\dagger$. We use the definition for chiral fields $\Psi_{L,R}^c = (\Psi_{L,R})^c = C\overline{\Psi_{L,R}}^T = P_{R,L}\Psi^c$, with $P_{R,L} = (1 \pm \gamma_5)/2$. Furthermore, $L = (\nu_L, e_L)^T$ is the left-handed lepton doublet and $\tilde{H} = i\tau_2 H^*$ with H the Higgs doublet

$$H = \frac{v}{\sqrt{2}} U(x) \begin{pmatrix} 0 \\ 1 + \frac{h(x)}{v} \end{pmatrix}. \tag{2.2}$$

Here $v = 246\,\text{GeV}$ is the Higgs vacuum expectation value (vev), $h(x)$ is the Higgs field, and $U(x)$ is an SU(2) matrix encoding the Goldstone modes. Generally, ν_R is a column vector of n right-handed sterile neutrinos, making Y_ν a $3 \times n$ matrix of Yukawa couplings and $\bar{M}_R$ a symmetric complex $n \times n$ mass matrix. We will work in the basis where the charged leptons $e^i_{L,R}$ and quarks $u^i_{L,R}$ and d^i_R are mass eigenstates ($i = 1,2,3$). After electroweak symmetry breaking this then gives $d^i_L = V^{ij} d^{j,\,\text{mass}}_L$, where V is the CKM matrix. We discuss the mass and flavor bases for the neutrinos in the next subsection.

Finally, the relevant dimension-five operators can be written as,

$$\mathcal{L}^{(\bar{5})}_{\nu_L} = \epsilon_{kl}\epsilon_{mn}(L^T_k\, C^{(5)}\, CL_m)H_l H_n\,, \qquad \mathcal{L}^{(\bar{5})}_{\nu_R} = -\bar{\nu}^c_R\, \bar{M}^{(5)}_R \nu_R H^\dagger H\,, \qquad (2.3)$$

while the needed dimension-six operators involving left- and right-handed neutrinos are collected in tables 3 and 4 of appendix A, respectively.

2.1 The Lagrangian below the electroweak scale

Below the electroweak scale the Lagrangian of eq. (2.1) induces the following mass terms for the neutrinos,

$$\mathcal{L}_m = -\frac{1}{2}\bar{N}^c M_\nu N + \text{h.c.}\,, \qquad M_\nu = \begin{pmatrix} M_L & M^*_D \\ M^\dagger_D & M^\dagger_R \end{pmatrix}\,, \qquad (2.4)$$

where $M_L = -v^2 C^{(5)}$, $M_D = \frac{v}{\sqrt{2}}\left[Y_\nu - \frac{v^2}{2}C^{(6)}_{L\nu H}\right]$, and $M_R = \bar{M}_R + v^2 \bar{M}^{(5)}_R$. Furthermore, $N = (\nu_L,\, \nu^c_R)^T$ and M_ν is a $N \times N$ symmetric matrix, with $N = 3 + n$. This matrix can be diagonalized by an $N \times N$ unitary matrix, U,

$$U^T M_\nu U = m_\nu = \text{diag}(m_1, \ldots, m_{3+n})\,, \qquad N = U N_m\,. \qquad (2.5)$$

This allows us to write the kinetic and mass terms of the neutrinos in the simple form

$$\mathcal{L}_\nu = \frac{1}{2}\bar{\nu} i\slashed{\partial}\nu - \frac{1}{2}\bar{\nu} m_\nu \nu\,, \qquad (2.6)$$

in terms of the Majorana mass eigenstates $\nu = N_m + N^c_m = \nu^c$. These eigenstates are related to the flavor basis by

$$\begin{aligned}
\nu_L &= P_L(PU)\nu\,, & \nu^c_L &= P_R(PU^*)\nu\,, \\
\nu_R &= P_R(P_s U^*)\nu\,, & \nu^c_R &= P_L(P_s U)\nu\,,
\end{aligned} \qquad (2.7)$$

where P and P_s are $3 \times N$ and $n \times N$ projector matrices

$$P = \begin{pmatrix} \mathcal{I}_{3\times 3} & 0_{3\times n} \end{pmatrix}\,, \qquad P_s = \begin{pmatrix} 0_{n\times 3} & \mathcal{I}_{n\times n} \end{pmatrix}\,, \qquad (2.8)$$

which project onto the active and sterile states, respectively.

We can use the above to write the charged-current interactions, which are induced by the dimension-six operators in eq. (2.1) below the electroweak scale, in the mass basis of

the neutrinos. In the notation of ref. [23], this gives, at the scale $\mu \simeq 2\,\text{GeV}$,

$$
\begin{aligned}
\mathcal{L}^{(6)} = \frac{2G_F}{\sqrt{2}} \Bigg\{ &\bar{u}_L\gamma^\mu d_L \left[\bar{e}_R\gamma_\mu C^{(6)}_{\text{VLR}}\,\nu + \bar{e}_L\gamma_\mu C^{(6)}_{\text{VLL}}\,\nu \right] + \bar{u}_R\gamma^\mu d_R \left[\bar{e}_R\,\gamma_\mu C^{(6)}_{\text{VRR}}\,\nu + \bar{e}_L\,\gamma_\mu C^{(6)}_{\text{VRL}}\,\nu \right] \\
&+ \bar{u}_L d_R \left[\bar{e}_L\,C^{(6)}_{\text{SRR}}\nu + \bar{e}_R\,C^{(6)}_{\text{SRL}}\nu \right] + \bar{u}_R d_L \left[\bar{e}_L\,C^{(6)}_{\text{SLR}}\nu + \bar{e}_R\,C^{(6)}_{\text{SLL}}\nu \right] \\
&+ \bar{u}_L\sigma^{\mu\nu}d_R\,\bar{e}_L\sigma_{\mu\nu}C^{(6)}_{\text{TRR}}\,\nu + \bar{u}_R\sigma^{\mu\nu}d_L\,\bar{e}_R\sigma_{\mu\nu}C^{(6)}_{\text{TLL}}\,\nu \Bigg\} + \text{h.c.}
\end{aligned} \tag{2.9}
$$

The matching of the above coefficients to those in eq. (2.1) is described in appendix A. In the SM, only the $C^{(6)}_{\text{VLL}}$ coefficient is nonzero. In the limit of vanishing neutrinos masses, the couplings $C^{(6)}_{\Gamma AL}$, with $\Gamma = \{V, S, T\}$ and $A = \{L, R\}$, are induced by the dimension-six interactions involving left-handed neutrinos in $\mathcal{L}^{(\bar{6})}_{\nu_L}$, while $C^{(6)}_{\Gamma AR}$ are induced by the operators involving right-handed neutrinos in $\mathcal{L}^{(\bar{6})}_{\nu_R}$.[2]

Eq. (2.9) provides the interactions that are relevant for both single- and double-β decays. As such, the above Lagrangian has been studied extensively in the literature in the context of β decays, although usually using a different convention. We provide the translation to the notation of ref. [8] in table 1. Since β decays are low-energy observables, they are commonly described in terms of the interactions involving nucleons instead of the quark-level interactions given above. The Lagrangian, often used in studies of β decays, is then written in the following form:[3]

$$
\begin{aligned}
\mathcal{L}_{\text{Lee-Yang}} = &-\bar{p}\gamma^\mu n \left(\bar{e}_L\gamma_\mu C^+_V\nu + \bar{e}_R\gamma_\mu C^-_V\nu \right) - \bar{p}\gamma^\mu\gamma_5 n \left(\bar{e}_L\gamma_\mu C^+_A\nu - \bar{e}_R\gamma_\mu C^-_A\nu \right) \\
&- \bar{p}n \left(\bar{e}_R C^+_S\nu + \bar{e}_L C^-_S\nu \right) - \frac{1}{2}\bar{p}\sigma^{\mu\nu}n \left(\bar{e}_R\sigma_{\mu\nu}C^+_T\nu + \bar{e}_L\sigma_{\mu\nu}C^-_T\nu \right) \\
&+ \bar{p}\gamma_5 n \left(\bar{e}_R C^+_P\nu - \bar{e}_L C^-_P\nu \right) + \text{h.c.}
\end{aligned} \tag{2.10}
$$

In our analysis, we will focus on the couplings to neutrinos with right-handed chirality, corresponding to the couplings, $C^-_{V,A,S,P,T}$ in the above Lagrangian, or $C^{(6)}_{\Gamma AR}$ of eq. (2.9). Given the matching discussed in appendix A, the relevant couplings are all induced by interactions that involve sterile neutrinos.[4]

From the above Lagrangian one can already see the form of the contributions to single-β decay and $0\nu\beta\beta$. The contributions to β decay take the form $\Gamma_\beta \sim \sum_{\alpha,\beta} \sum_{i=1}^N [C_\alpha]_{ei} [C_\beta]^*_{ei}$ $\Gamma_{\alpha\beta}(m_i)$, where $\Gamma_{\alpha\beta}(m_i)$ depends on the Wilson coefficients, $C_{\alpha,\beta}$, under consideration and is nearly independent of m_i for small neutrino masses, $m_i \ll Q$. In this case, the contributions through the SM charged current reduce to $\Gamma^{\text{SM}}_\beta \sim \sum_{i=1}^N |U_{ei}|^2 \Gamma(m_i) \simeq \Gamma(0)$ and

---

[2] As can be seen from the matching in appendix A, this is no longer true for nonzero $M_{D,R}$ as these terms allow for chirality flips of the neutrino fields.

[3] The $C^\pm_\alpha$ couplings of ref. [8] are defined in the flavor basis and thus related to those used here by the change of basis in eq. (2.7). In our numerical analyses, we will often focus on the case with $n = 1$ and $U_{4\alpha} = \delta_{4\alpha}$ for simplicity. In this scenario the C^-_α couplings used here coincide with those of FGN.

[4] Note that these interactions can also be induced by operators involving left-handed neutrinos once one considers operators of dimension seven, since ν^c_L is right handed. However, such operators violate lepton number by two units and are already stringently constrained by $0\nu\beta\beta$, leading to $\Lambda > 10\,\text{TeV}$ [24]. This implies their effects are unlikely to be measured in β experiments, given the sensitivity to the C^-_i couplings.

$C_{\text{VLL}}^{(6)} = -2V_{ud}(1 + \epsilon_L)$	$C_{\text{VLR}}^{(6)} = -2V_{ud}\,\tilde{\epsilon}_L$
$C_{\text{VRL}}^{(6)} = -2V_{ud}\,\epsilon_R$	$C_{\text{VRR}}^{(6)} = -2V_{ud}\,\tilde{\epsilon}_R$
$C_{\text{SLL}}^{(6)} = -V_{ud}(\epsilon_S + \epsilon_P)$	$C_{\text{SLR}}^{(6)} = -V_{ud}(\tilde{\epsilon}_S + \tilde{\epsilon}_P)$
$C_{\text{SRL}}^{(6)} = -V_{ud}(\epsilon_S - \epsilon_P)$	$C_{\text{SRR}}^{(6)} = -V_{ud}(\tilde{\epsilon}_S - \tilde{\epsilon}_P)$
$C_{\text{TLL}}^{(6)} = -\frac{1}{2}V_{ud}\,\epsilon_T$	$C_{\text{TRR}}^{(6)} = -\frac{1}{2}V_{ud}\,\tilde{\epsilon}_T$

Table 1. Translation to the notation of [8].

are independent of neutrinos masses and mixings. For large m_i the partial rates $\Gamma_{\alpha\beta}(m_i)$ depend more sensitively on the neutrino masses until they vanish for $m_i > Q$, as the decay to ν_i becomes energetically disallowed. This effect can be searched for experimentally by looking for kinks in the electron spectrum [25, 26].

Instead, the $0\nu\beta\beta$ decay rate is an LNV observable and therefore requires an explicit insertion of the neutrino mass leading to, $\Gamma_{0\nu\beta\beta} \sim \left| \sum_{\alpha,\beta} \sum_{i=1}^{N} [C_\alpha]_{ei}\, m_i\, [C_\beta]_{ei}\, \mathcal{A}_{\alpha\beta}(m_i) \right|^2$. Similar to β decay, the amplitudes $\mathcal{A}_{\alpha\beta}(m_i)$ depend on the Wilson coefficients under consideration and are nearly independent of m_i for small neutrino masses, $m_i \ll m_\pi$. For large neutrino masses, the amplitudes scale as $\mathcal{A}_{\alpha\beta}(m_i) \sim 1/m_i^2$, with a more complicated dependence in between, see section 3.2 and ref. [23] for more details.

The relation between the parameters in eq. (2.10) and those in table 1 is given by [5]

$$
\begin{aligned}
C_V^+ &= \frac{V_{ud}}{v^2} g_V \sqrt{1 + \Delta_R^V}(1 + \epsilon_L + \epsilon_R), & C_V^- &= \frac{V_{ud}}{v^2} g_V \sqrt{1 + \Delta_R^V}(\tilde{\epsilon}_L + \tilde{\epsilon}_R), \\
C_A^+ &= -\frac{V_{ud}}{v^2} g_A \sqrt{1 + \Delta_R^A}(1 + \epsilon_L - \epsilon_R), & C_A^- &= \frac{V_{ud}}{v^2} g_A \sqrt{1 + \Delta_R^A}(\tilde{\epsilon}_L - \tilde{\epsilon}_R), \\
C_T^+ &= \frac{V_{ud}}{v^2} g_T \epsilon_T, & C_T^- &= \frac{V_{ud}}{v^2} g_T \tilde{\epsilon}_T, \\
C_S^+ &= \frac{V_{ud}}{v^2} g_S \epsilon_S, & C_S^- &= \frac{V_{ud}}{v^2} g_S \tilde{\epsilon}_S, \\
C_P^+ &= \frac{V_{ud}}{v^2} g_P \epsilon_P, & C_P^- &= -\frac{V_{ud}}{v^2} g_P \tilde{\epsilon}_P, \quad (2.11)
\end{aligned}
$$

where $g_{V,A,S,P,T}$ are the vector, axial, scalar, pseudoscalar, and tensor charges of the nucleon [5], which can be determined using lattice calculations. Here, $g_V = 1$ up to (negligible) quadratic corrections in isospin-symmetry breaking [27] and we use the FLAG'19 averages [28] for the axial, scalar and tensor charges: $g_A = 1.251(33)$, $g_S = 1.022(100)$ and $g_T = 0.989(33)$ [29, 30] (see also ref. [31]). Although the pseudoscalar charge is enhanced by the pion pole, namely $g_P = 349(9)$ [31], the suppression of the pseudoscalar contributions to single β-decay is larger such that β-decay experiments do not significantly constrain C_P^-.

The matching in eq. (2.11) includes the short-distance (inner) radiative corrections Δ_R^V and Δ_R^A. Especially the former is important, because it is necessary to extract V_{ud} from nuclear data. Four recent calculations of this quantity are available [32–35], which all agree within 1σ. In this analysis we use the Seng et al. evaluation, $\Delta_R^V = 0.02467(22)$ [32], which has the smallest uncertainty. Given the assumption about the reality of ϵ_X and $\tilde{\epsilon}_X$, all $C_X^\pm$ are then also real.

3 Single- and neutrinoless double-β decay observables

3.1 Single β-decay

As mentioned the interactions in eq. (2.10) give tree-level corrections to the SM charged current which can be probed in β decays. We will follow the analysis of ref. [8] to constrain the couplings in eq. (2.10).[5] Here we briefly summarize this analysis by FGN and discuss some of the details, related to theory uncertainties, of the fit.

Since the observables considered by FGN include the β decays of the neutron as well as nuclei, the theoretical expressions depend of the NMEs in addition to the hadronic matrix elements appearing in eq. (2.11). At leading order, nuclear effects are encapsulated in the so-called Fermi (F) and Gamow-Teller (GT) matrix elements, $M_{F,GT}$. Leading-order expressions for beta decay observables in terms of the Lee-Yang Wilson coefficients $C_X^{\pm}$ can be found in refs. [36, 37]. However, given the experimental precision, subleading effects such as weak-magnetism and long-distance electromagnetic corrections have to be included in the SM terms. These small contributions can be calculated with high accuracy for the transitions that are included in this work [3, 38–40].

Apart from the corrections that can be accurately determined, there are several places where theoretical uncertainties are sizable. In particular, the "polluted" mixing parameters, $\tilde{\rho}_i$, of [8] involve ratios of GT to F matrix elements which have not been calculated to sufficient precision. They are therefore treated as nuisance parameters and are marginalized over in the fit. Furthermore, theoretical uncertainties related to the nuclei-dependent parts of the radiative corrections is taken into account by including two additional nuisance parameters, $\eta_{2,3}$ [8].

In ref. [8], the best-fit results are obtained by marginalizing over nuisance parameters and other Wilson coefficients. In this study, depending on the scenario under consideration, we do not always marginalize over all the Wilson coefficients. In some cases we keep certain Wilson coefficients fixed, in order to be able to compare directly with the $0\nu\beta\beta$ limits. As a result, the β limits we present are not always identical to those presented in ref. [8]. We do always marginalize over all the nuisance parameters, even when only turning on one or two Wilson coefficients at a time.

Finally, although FGN neglected all neutrino masses, a complete analysis would in principle include the effects that the neutrino masses, m_i, have on single-β observables. Instead of taking into account the full m_i dependence of all β-decay observables in the fit, we will restrict ourselves to a range of m_i for which the FGN analysis is still applicable. We estimate an upper bound on this range by considering the ways in which β observables will receive corrections due to nonzero m_i. First, the contributions induced by the SM charged current are proportional to $\sum_{i=1}^{N} |U_{ei}|^2 = 1$ for negligible neutrino masses, with corrections of the form[6] $\sum_{i=1}^{N} |U_{ei}|^2 \frac{m_i^2}{Q^2}$. Here, the Q values of the isotopes that appear in the fit are in the MeV range, $Q \gtrsim 0.7\,\text{MeV}$. Combining this with the upper limit on the mixing parameter U_{e4}, roughly $|U_{e4}|^2 < 10^{-3}$ for $m_4 = 100\,\text{keV}$ from the β-decay

---

[5]We thank Adam Falkowski and Martín González-Alonso for providing us with the χ^2 function used in the analysis of ref. [8].

[6]An explicit calculation of the β decay rate confirms this scaling.

spectrum of ^{35}S [18, 25, 41], the corrections to the β decay rates due to a fourth neutrino are expected to be below the $\mathcal{O}(10^{-4})$ level, for $m_4 \lesssim 100\,\text{keV}$. In addition, the contributions of dimension-six operators will receive corrections $\sim \frac{m_i^2}{Q^2}|v^2 C_\alpha^-|^2$, or, allowing for interference, $\sim \frac{m_i}{Q}|U_{e4}\,v^2 C_\alpha^-|$. Since the higher-dimensional operators will be suppressed compared to the SM, $v^2 C_\alpha^- \lesssim 0.1$, we expect these corrections to contribute at most at the $\mathcal{O}(10^{-4})$ level. The observables in the FGN analysis, such as phase-space corrected lifetimes ($\mathcal{F}t$ values) and β-decay asymmetries, have $\mathcal{O}(10^{-3})$ uncertainties and are thus not sensitive to neutrino-mass corrections for $m_4 \lesssim 100\,\text{keV}$.

3.2 Neutrinoless double beta decay

We now turn to the calculation of $0\nu\beta\beta$ decay rates of various nuclear isotopes. We closely follow the framework of ref. [23]. Our starting point is the following effective Lagrangian of eq. (2.9)

$$
\mathcal{L}^{(6)} = \frac{2G_F}{\sqrt{2}} \Bigg\{ \bar{u}_L \gamma^\mu d_L \left[\bar{e}_L \gamma_\mu C_{\text{VLL}}^{(6)}\, \nu + \bar{e}_R \gamma_\mu C_{\text{VLR}}^{(6)}\, \nu \right] + \bar{u}_R \gamma^\mu d_R \left[\bar{e}_R\, \gamma_\mu C_{\text{VRR}}^{(6)}\, \nu \right]
$$
$$
+ \bar{u}_L d_R \left[\bar{e}_L\, C_{\text{SRR}}^{(6)} \nu \right] + \bar{u}_R d_L \left[\bar{e}_L\, C_{\text{SLR}}^{(6)} \nu \right] + \bar{u}_L \sigma^{\mu\nu} d_R\, \bar{e}_L \sigma_{\mu\nu} C_{\text{TRR}}^{(6)}\, \nu \Bigg\} + \text{h.c.} \quad (3.1)
$$

This Lagrangian is written in the neutrino mass basis where ν denotes a $3+n$ column vector of neutrino mass eigenstates. The Lagrangian is defined at a scale $\mu = 2\,\text{GeV}$ and consists of operators that can be induced by operators of the dimension-six νSMEFT Lagrangian involving one ν_R field. The only exception is the $C_{\text{VLL}}^{(6)}$ term which also includes the SM charged weak interaction of the active neutrinos.

We consider a simplified scenario where $n = 1$ implying a single sterile neutrino with arbitrary mass m_4. While a pure $3 + 1$ model (without dimension-five operators) would lead to two massless neutrinos, we assume some mass mechanism for the active neutrinos for instance through additional decoupled sterile neutrinos. As discussed above, we focus on m_4 masses well below the MeV scale when comparing to single-β experiments, where (in most cases) such neutrinos can be treated as massless,[7] while we consider larger masses when investigating the reach of $0\nu\beta\beta$ experiments.

Under these assumptions it is possible to write down a relatively simple expression for the $0\nu\beta\beta$ decay rate

$$
\left(T_{1/2}^{0\nu} \right)^{-1} = g_A^4 \Bigg\{ G_{01} \left(|\mathcal{A}_L|^2 + |\mathcal{A}_R|^2 \right) - 2(G_{01} - G_{04})\text{Re}\mathcal{A}_L^* \mathcal{A}_R
$$
$$
+ G_{09}\, |\mathcal{A}_M|^2 + G_{06}\, \text{Re}\left[(\mathcal{A}_L - \mathcal{A}_R)\mathcal{A}_M^*\right] \Bigg\}, \quad (3.2)
$$

in terms of electron phase-space factors, G_{0i}, and three so-called subamplitudes $\mathcal{A}_{L,R,M}$. The G_{0i} phase space factors are defined in ref. [24] and have been calculated in the literature [45–47]. They include Coulomb corrections between the outgoing electrons and the nucleus and the (partial) screening effect of the nuclear charge by the surrounding electron cloud. Numerical values are given in table 2.

---

[7]Exceptions are experiments, such as KATRIN, aiming to directly measure the neutrino mass [42–44].

[47]	^{76}Ge	^{82}Se	^{130}Te	^{136}Xe
G_{01}	0.22	1.	1.4	1.5
G_{04}	0.19	0.86	1.1	1.2
G_{06}	0.33	1.1	1.7	1.8
G_{09}	0.48	2.	2.8	2.8
Q/MeV [48]	2.04	3.0	2.5	2.5

Table 2. Phase space factors in units of 10^{-14} yr^{-1} obtained in ref. [47]. The last row shows the Q value of $0\nu\beta\beta$ for various isotopes, where $Q = M_i - M_f - 2m_e$.

The subamplitudes depend on the underlying LNV mechanism (in our case, the Majorana mass terms and the non-standard neutrino couplings) as well as hadronic and nuclear matrix elements. Each subamplitude is written as a sum over neutrino mass eigenstates

$$\mathcal{A}_{L,R,M} = \sum_{i=1}^{3+n} \mathcal{A}_{L,R,M}(m_i). \tag{3.3}$$

Strictly speaking this description is only valid if $m_i < 1\,\text{GeV}$ or so. Heavier neutrinos must be integrated out leading to effective dimension-nine interactions which give additional contributions in eq. (3.3). In what follows we capture these effects by demanding that the m_i-dependent nuclear and hadronic matrix elements have the correct m_i behavior to reproduce the amplitudes that would result from integrating out the neutrinos at the quark level, in the $m_i \gg 1\,\text{GeV}$ region. As we focus on neutrino masses smaller than a GeV or so, we relegate a discussion of the procedure to appendix B and refer to ref. [23] for more details.

The first subamplitude is given by

$$\begin{aligned}
\mathcal{A}_L(m_i) = -\frac{m_i}{4m_e} \Bigg\{ & [\mathcal{M}_V(m_i) + \mathcal{M}_A(m_i)] \left(C_{\text{VLL}}^{(6)}\right)_{ei}^2 \\
& + \mathcal{M}_{PS}(m_i) \left[\frac{B^2}{m_\pi^2} \left(C_{\text{SRR}}^{(6)} - C_{\text{SLR}}^{(6)}\right)_{ei} - 2\frac{B}{m_i} \left(C_{\text{VLL}}^{(6)}\right)_{ei} \right] \left(C_{\text{SRR}}^{(6)} - C_{\text{SLR}}^{(6)}\right)_{ei} \\
& + \mathcal{M}_S(m_i) \left(C_{\text{SRR}}^{(6)} + C_{\text{SLR}}^{(6)}\right)_{ei}^2 - \mathcal{M}_T(m_i) \left(C_{\text{TRR}}^{(6)}\right)_{ei}^2 \\
& + \frac{m_N}{m_i} \mathcal{M}_{TV}(m_i) \left(C_{\text{VLL}}^{(6)}\right)_{ei} \left(C_{\text{TRR}}^{(6)}\right)_{ei} \Bigg\} + \mathcal{A}_L^{(\nu)}(m_i), \tag{3.4}
\end{aligned}$$

in terms of the low-energy constant (LEC) $B \simeq 2.7\,\text{GeV}$, m_N and m_π the nucleon and pion mass, respectively, and various combinations of neutrino-mass-dependent NMEs $\mathcal{M}_I(m_i)$ which are discussed below. Most terms in the expression for $\mathcal{A}_L(m_i)$ have an explicit m_i dependence accounting for the required lepton number violation. Two interference terms, linear in $\left(C_{\text{VLL}}^{(6)}\right)_{ei}$, seem to violate this scaling. However, in order for the product with $\left(C_{\text{SRR}}^{(6)} - C_{\text{SLR}}^{(6)}\right)_{ei}$ or $\left(C_{\text{TRR}}^{(6)}\right)_{ei}$ to be non-vanishing, $C_{\text{VLL}}^{(6)}$ requires an insertion of M_R, see the last term in eq. (A.1), so that the relevant terms $\left(C_{\text{VLL}}^{(6)}\right)_{ei} \sim m_i v/\Lambda^2$ scale

linearly in the Majorana mass. These interference terms are then effectively suppressed by $B/v \sim m_N/v = \mathcal{O}(10^{-2})$ and can be neglected.

The term $\mathcal{A}_L^{(\nu)}(m_i)$ describes contributions from the exchange of hard neutrinos, virtual neutrinos with momenta $\gtrsim$ GeV. Such contributions lead to $\mathcal{O}(1)$ corrections to the amplitudes, but in most cases depend on QCD matrix elements that are not well known. For our numerical analysis we have used lattice QCD determinations [49] when possible, while the remaining matrix elements are estimated using naive dimensional analysis (NDA), see appendix B and ref. [23] for more details.

Similarly

$$\mathcal{A}_R(m_i) = -\frac{m_i}{4m_e}\left\{\mathcal{M}_V(m_i)\left(C_{\mathrm{VRR}}^{(6)} + C_{\mathrm{VLR}}^{(6)}\right)_{ei}^2 + \mathcal{M}_A(m_i)\left(C_{\mathrm{VRR}}^{(6)} - C_{\mathrm{VLR}}^{(6)}\right)_{ei}^2\right\}$$
$$+ \mathcal{A}_R^{(\nu)}(m_i)\,, \tag{3.5}$$

while the final subamplitude contains only interference terms

$$\mathcal{A}_M(m_i) = -\frac{m_i}{2m_e}\left\{\frac{m_N}{m_i}\mathcal{M}_{VA}(m_i)\left(C_{\mathrm{VLL}}^{(6)}\right)_{ei}\left(C_{\mathrm{VLR}}^{(6)}\right)_{ei}\right.$$
$$+ \frac{1}{2}\mathcal{M}_S(m_i)\frac{g_V}{g_S}\left(C_{\mathrm{VRR}}^{(6)} + C_{\mathrm{VLR}}^{(6)}\right)_{ei}\left(C_{\mathrm{SRR}}^{(6)} + C_{\mathrm{SLR}}^{(6)}\right)_{ei}$$
$$+ \mathcal{M}_{TA}(m_i)\left(C_{\mathrm{VRR}}^{(6)} - C_{\mathrm{VLR}}^{(6)}\right)_{ei}\left(C_{\mathrm{TRR}}^{(6)}\right)_{ei}\right\} + \mathcal{A}_M^{(\nu)}(m_i)\,. \tag{3.6}$$

Here the $\mathcal{A}_{R,M}^{(\nu)}(m_i)$ subamplitudes are again due to the exchange of hard neutrinos, which we discuss in appendix B.

As mentioned, the $\mathcal{M}_I(m_i)$ are linear combinations of different NMEs which are discussed in appendix B. These elements in principle depend on the mass of the neutrino that is being exchanged. However, for neutrino masses below a few MeV, this mass dependence can be safely neglected. The mass-independent NMEs, $\mathcal{M}_I(0)$, have been calculated with various nuclear methods. A collection of results is given in appendix B, table 5 for several isotopes. The differences between nuclear calculations lead to an additional $\mathcal{O}(1)$ uncertainty on the $0\nu\beta\beta$ decay results [50].

For heavier neutrino masses, the mass dependence of the NMEs and hadronic low-energy constants cannot be neglected. We follow the approach of ref. [23] which interpolates between regions where $m_i \ll k_F \sim m_\pi$ where k_F is the typical Fermi momentum in nuclei and $m_i > \Lambda_\chi \sim 1\,\mathrm{GeV}$ where neutrinos can be integrated out at the quark level leading to local LNV operators. In the small-mass regime, NMEs and LECs are essentially mass independent and the amplitude scales linearly with m_i. In the large-mass regime, the neutrino mass-dependence is captured by the Wilson coefficients of dimension-nine operators, $\sim (\bar{u}d)^2\bar{e}e^c$, that are generated after integrating out the neutrinos. The Wilson coefficients then have the form $C_\alpha^{(6)}C_\beta^{(6)}/m_i$ so that the amplitude scales as $1/m_i$, while the NMEs and LECs are again mass independent. The mass dependence in the intermediate regime arises from two sources: 1) the neutrino propagator scales as $m_i/(\mathbf{q}^2 + m_i^2)$ instead

of the Coulomb-like $m_i/|\mathbf{q}|$, 2) LECs associated to the exchange of hard virtual neutrinos pick up an intrinsic m_i dependence. Here we will apply the formulae that were constructed in ref. [23] by matching to results in the low- and high-mass regimes and interpolating in between. These formulae thus have the largest uncertainty in the $m_i \sim \Lambda_\chi$ regime where the chiral and perturbative-QCD descriptions cannot be trusted, see appendix B for explicit expressions.

4   Results

We now turn to the calculation of $0\nu\beta\beta$ constraints on the various effective interactions. We begin our analysis by considering a single C_X^- coupling, while setting the remaining Wilson coefficients to their SM values. We compare the constraints from $0\nu\beta\beta$ decay against single-β limits [8]. The former are only valid for Majorana neutrinos. The latter are strictly speaking only valid in the limit of massless neutrinos but we will consider neutrino masses $m_{\nu_R} < 100\,\text{keV}$, where this is a reasonable approximation, see the discussion in section 3.1.

To derive the contributions of the scenarios considered below to $0\nu\beta\beta$ we make several assumptions. We will consider a case with one additional neutrino, $n = 1$, and assume that the non-standard interactions only couple to the sterile state, $i = 4$ (this is equivalent to assuming there is no mixing between sterile and active neutrinos, $U_{4i} \propto \delta_{4i}$). In addition, we will not consider the 'usual' mechanism for inducing $0\nu\beta\beta$ proportional to $m_{\beta\beta} = m_i U_{ei}^2$. Both simplifications neglect additional contributions to $0\nu\beta\beta$; while the neglected mixing effects can only contribute through interference terms and will tend to be suppressed (see section 3.2), the $\sim m_{\beta\beta}$ terms can in principle be sizable. The reason we nevertheless make these simplifications is that these effects depend on the details of the neutrino masses and mixings, determined by $M_{L,D,R}$ in eq. (2.4), which can only be assessed in a full model of neutrino masses. Barring cancelations, these additional contributions will tend to increase the predicted $0\nu\beta\beta$ rate, thereby strengthening the limits presented here. Our approach is thus conservative.

4.1   Single coupling analysis

Our results are shown in figures 1 and 2 for the 5 different couplings. The plots depict the $m_4 - v^2 C_i^-$ plane, where the blue (red) shaded areas show the parameter space allowed by the single-β (double-β) constraints. To obtain the latter we assume there are no significant cancelations between the ν_R contributions and those proportional to $m_{\beta\beta}$. The width of the $0\nu\beta\beta$ bands show the variation induced by using shell-model [51] or quasi-particle random phase approximation (QRPA) [52] NMEs, illustrating the impact of the nuclear theory uncertainties. The panels do not show the effect of changes in the LECs discussed in appendix B.2, significant uncertainties of which would lead to additional errors at the $\mathcal{O}(1)$ level. For reference we also show the LHC limits and, for C_P^-, the constraint from $\Gamma(\pi \to e\nu)/\Gamma(\pi \to \mu\nu)$ in green [2, 30]. The collider limits were derived from $pp \to e + \text{MET} + X$ based on 20(36) fm^{-1} data recorded at $\sqrt{s} = 8(13)\,\text{TeV}$ for the $C_{V,A}^-$ ($C_{S,T}^-$) couplings. In all cases the present KAMLAND-Zen limit are sensitive to couplings $v^2 C_i^- < 1$ for sterile masses larger than about $1\,\text{eV}$. The $0\nu\beta\beta$ constraints become competitive
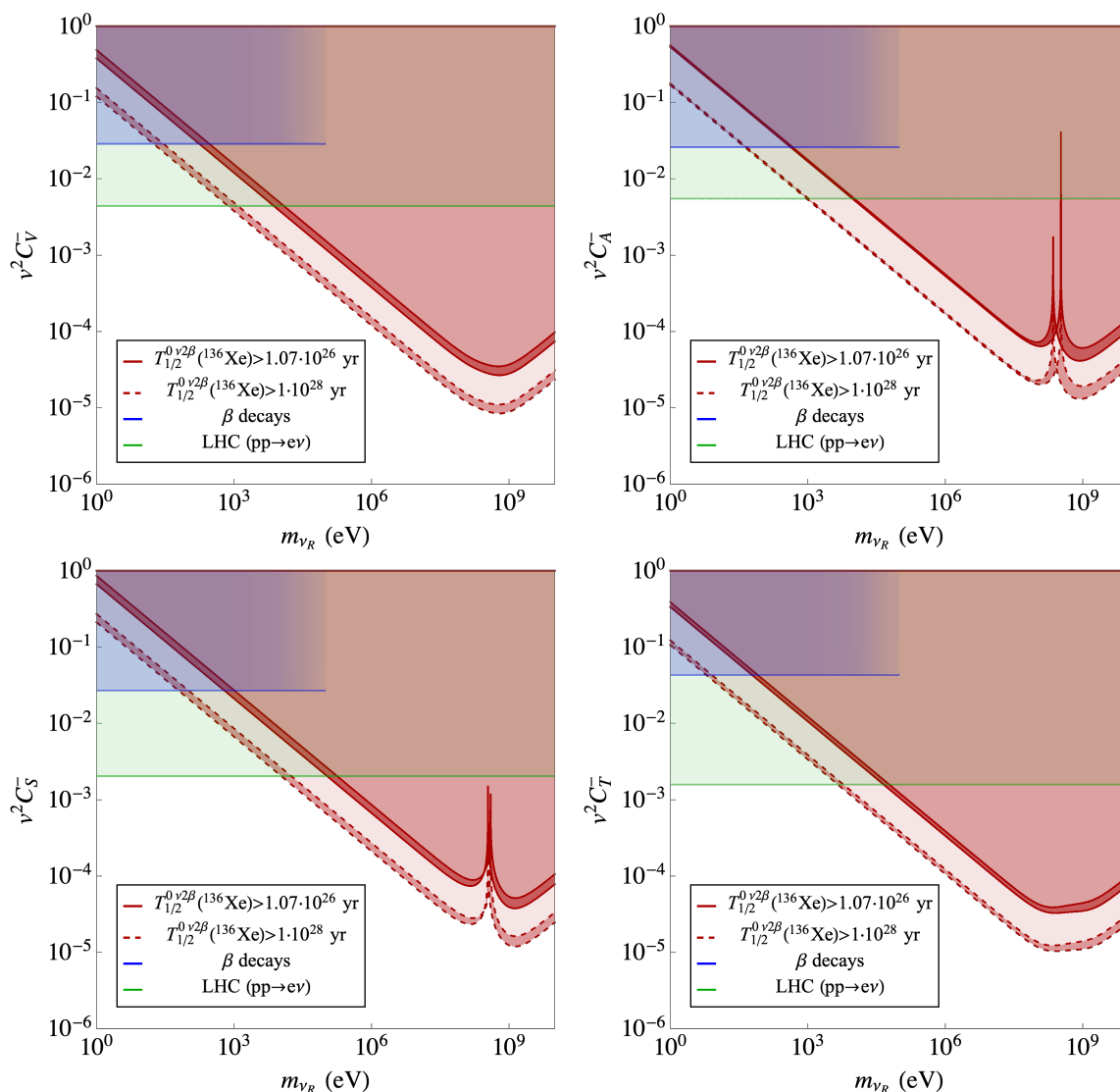
Figure 1. 90% C.L. limits from the $0\nu\beta\beta$ decay of ^{136}Xe (red) compared to a fit of β decays (blue) in the scenario where only one of the $v^2 C_i^-$ has been turned on. The width of the $0\nu\beta\beta$ bands indicate the variation induced by using shell-model [51] or QRPA [52] NMEs.

with those from single-β decay for masses larger than $\{180, 460, 610, 60\}$ eV in the case of $\{C_V^-, C_A^-, C_S^-, C_T^-\}$, respectively. Thus, if a nonzero value of $v^2 C_T^-$ at the $\mathcal{O}(0.01)$ level would be confirmed in β-decay experiments,[8] the present $0\nu\beta\beta$ limits imply that neutrinos are either Dirac particles or that $m_4 < 60$ eV.

The $0\nu\beta\beta$ decay bounds follow a slope $(C_i^-)^2 \sim 1/m_4$ for $m_4 < \mathcal{O}(100)$ MeV. This scaling changes to $(C_i^-)^2 \sim m_4$ for $m_4 > \mathcal{O}(2)$ GeV, with a more complicated mass dependence in between. The exact location of the peak sensitivity depends on the coupling under consideration because of non-trivial mass dependence of nuclear and QCD matrix

---

[8]The one-coupling fit roughly prefers nonzero values $|v^2 C_T^-| \in [0.01, 0.03]$ at 1σ. The significance grows when allowing all Wilson coefficients to be nonzero, see figure 4.
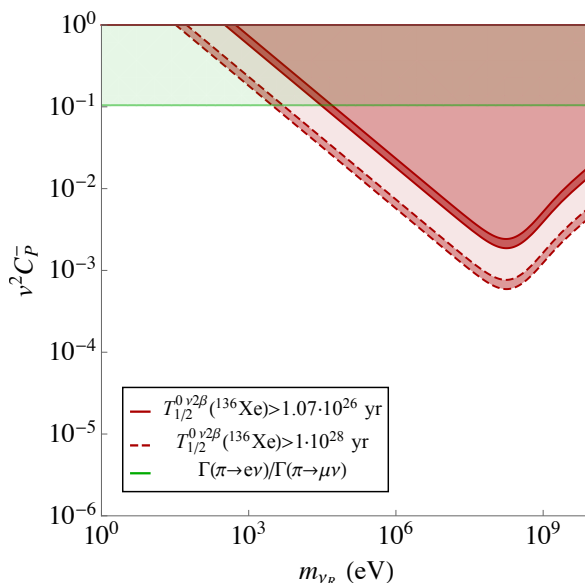
Figure 2. Same as figure 1 but for C_P^-.

elements. To get an idea of the sensitivity to BSM scales that are probed we can assume a typical scaling $C_i^- = 1/\Lambda^2$. The constraints on C_V^- then imply a BSM scale between $\Lambda > 0.7\,\text{TeV}$ for $m_4 = 10\,\text{eV}$ to a maximum sensitivity of $\Lambda > 47\,\text{TeV}$ for $m_4 = 0.5\,\text{GeV}$. These sensitivities should be compared to $\Lambda > 1.5\,\text{TeV}$ in the case of single-β decay. The dips that appear around $m_4 \sim \text{GeV}$ for C_A^- and C_S^- arise from the fact that the $0\nu\beta\beta$ decay rate vanishes. In these cases, for our particular choice of hadronic and nuclear matrix elements, the long-distance contributions cancel the short-distance terms. At this point, higher-order corrections should be included and our calculations are not reliable. Considering that this happens only for a tiny range of neutrino masses we do not pursue this further. Finally, we denote the prospective limit, $T_{1/2}^{0\nu\beta\beta} > 10^{28}\text{yr}$ from EXO-200 [53] by the dashed red lines. As this limit is a factor ~ 100 stronger than the current constraint, it leads to an improvement of $\sim \sqrt{10}$ on the C_i^- constraints.

The collider limits shown in figures 1 and 2 tend to be stronger than the single-β constraints by a factor of a few to an order of magnitude. However, the LHC limits from $pp \to e\nu$ only apply as long as the BSM physics responsible for the dimension-six interactions can still be treated as a contact interaction at high energies, i.e. as long as, $\Lambda \gg \sqrt{s} \sim \text{TeV}$. Instead, the limits from single- and double-β decay are subject to a milder assumption, $\Lambda \gg \text{GeV}$. In any case, if future LHC analyses find hints for interactions with light right-handed neutrinos, future $0\nu\beta\beta$ experiments should see a signal if the neutrinos are Majorana and have masses above roughly $1\,\text{keV}$.

Additional constraints on C_X^- arise from a careful analysis of the electron spectrum in neutrinoful double-β decay [54, 55]. In particular, the angular distribution of outgoing electrons in ^{100}Mo double-β decay [56], limits $\frac{v^2}{2}\left|\frac{C_V^-}{g_V} + \frac{C_A^-}{g_A}\right| \leq 0.03$ for $m_{\nu_R} < 0.1\,\text{MeV}$ comparable to the single-β decay bounds. Future experiments are expected to improve this to the 0.01 level [54]. We have not indicated these bounds in the plot.
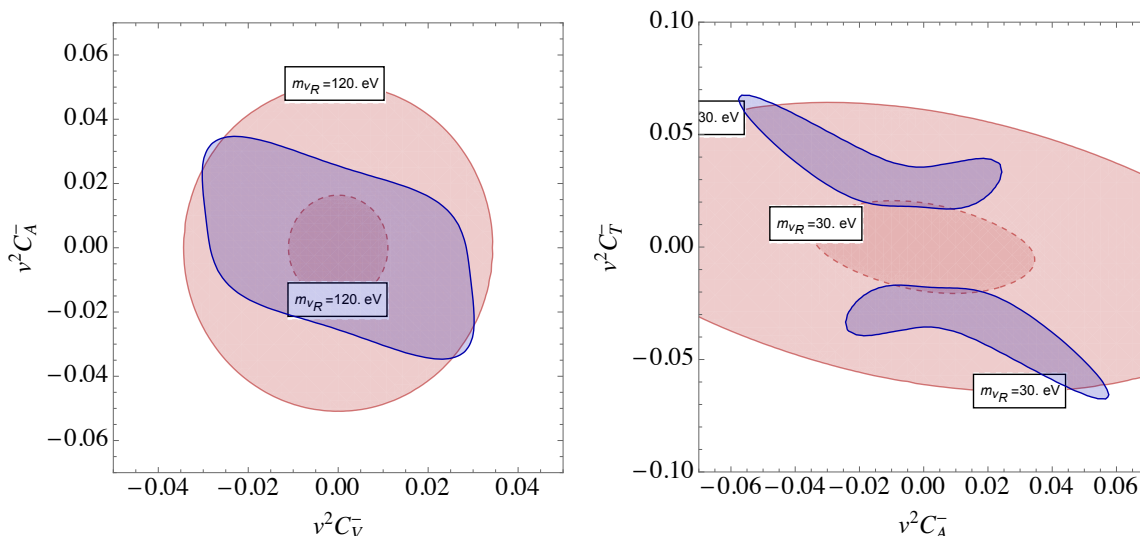
Figure 3. Exclusion plots showing $\Delta\chi^2 = 2.706$ contours in the $v^2 C_V^- \text{-} v^2 C_A^-$ and $v^2 C_A^- \text{-} v^2 C_T^-$ planes in the left and right panels, respectively. The blue (red) regions are those allowed by single-(double-)β decay constraints. In both cases we turned on only two Wilson coefficients at a time, setting the rest to their SM values.

As seen from figure 2, single-β decay experiments are not sensitive to C_P^- because of a Q^2/m_π^2 suppression of the amplitude where Q denotes the Q-value of the experiment. However, the ratio $\Gamma(\pi \to e\nu)/\Gamma(\pi \to \mu\nu)$ is rather sensitive to this coupling, leading to a stringent constraint that is overtaken by the $0\nu\beta\beta$ limit for $m_4 \gtrsim 30\,\text{keV}$.

4.2 Multi-coupling analysis

We now turn to a scenario where two couplings are turned on simultaneously, again setting the remaining couplings to their SM values. We focus on a comparison of single-β and $0\nu\beta\beta$ decay experiments. We show contours in the $v^2 C_V^- \text{-} v^2 C_A^-$ plane in the left panel of figure 3, corresponding to a case in which right-handed neutrinos couple to quarks through (axial) vector currents. The single-β bounds are depicted in blue and indicate good agreement with the SM expectation, which is represented by the origin. The blue contour resides within a square with boundaries $-0.03 < v^2 C_{A,V}^- < 0.03$. In the case of Majorana neutrinos, the (future) $0\nu\beta\beta$ constraints are shown by the (dashed) red contours, We again assumed there are no cancelations between the $\sim m_{\beta\beta}$ and non-standard contributions, while we used the NMEs of ref. [52] and neglected the $\mathcal{O}(1)$ hadronic and nuclear uncertainties. The bounds span an oval that can roughly be described by $\left(v^2 C_A^-\right)^2 + 2.2\left(v^2 C_V^-\right)^2 \lesssim 0.05 \times \frac{120\,\text{eV}}{m_4}$. The current $0\nu\beta\beta$ constraints are thus competitive with single-β probes for $m_4 > 200\,\text{eV}$ or so. Next-generation experiments will push this to $m_4 > 20\,\text{eV}$.

The right panel of figure 3 instead shows the $v^2 C_A^- \text{-} v^2 C_T^-$ plane where the (not too significant) discrepancy found in ref. [8] is visible. If this anomaly would be confirmed, the complementary nature of $0\nu\beta\beta$ could prove useful in identifying the nature and mass of right-handed neutrinos. With the current experimental $0\nu\beta\beta$ limits a nonzero value
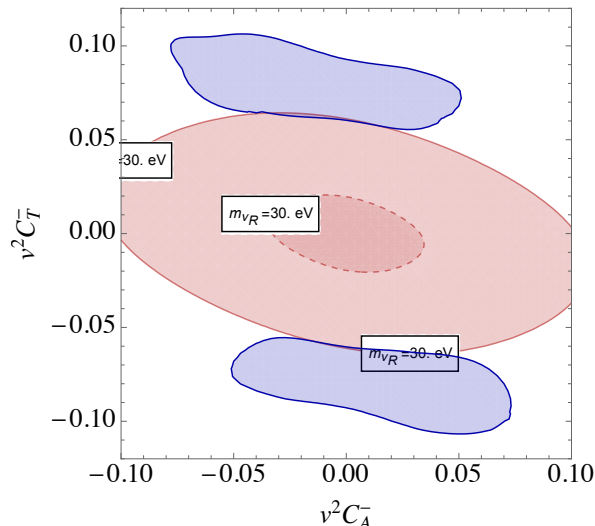
Figure 4. Similar to figure 3, however, here the single-β contours have been obtained by marginalizing over the other Wilson coefficients.

of $C_{A,T}^-$, consistent with the β-decay data, require neutrinos to be either Dirac or have masses below 300 eV. Next-generation $0\nu\beta\beta$ experiments will bring this down to 30 eV. Complementary constraints on neutrino masses in the eV range come from oscillation experiments [57, 58], while searches for kinks in the electron spectrum of single-β decay experiments [18, 25] are sensitive to masses up to the MeV range.

Finally, we use the same machinery to perform a fit of the β-decay data, where the single-β data is marginalized over all 5 couplings, while we only consider the $C_{A,T}^-$ contributions to $0\nu\beta\beta$. The resulting contour is shown in figure 4, which more clearly shows a preference for nonzero C_T^-. In this case, the preferred fit values of the Wilson coefficients are only consistent with Majorana neutrinos if the sterile neutrino has a mass below 30 eV. Next-generation experiments will push this 3 eV, covering essentially the entire possible mass range.

5 A leptoquark model

So far our analysis was performed purely in an EFT framework and we constrained effective couplings of the massive sterile neutrino. While this is convenient to demonstrate the complementarity between single-β and $0\nu\beta\beta$ experiments, it might also lead to oversimplifications. To get a sense of more realistic BSM scenarios that induce multiple dimension-six operators at the same time, we consider a toy model with several leptoquarks (LQs) that have interactions with right-handed neutrinos. Integrating out the leptoquarks leads to dimension-six νSMEFT operators [6].

Following the notation of ref. [59] we consider a BSM model with two scalar LQs, S_1 and $\tilde{R}_2$. S_1 has mass M_1 and transforms under $\mathrm{SU}(3)_c$ as an anti-triplet, under $\mathrm{SU}(2)_L$ as a singlet, and carries nonzero hypercharge: $S_1\left(\bar{\mathbf{3}}, \mathbf{1}, 1/3\right)$, while $\tilde{R}_2$ has mass M_2 and transforms under $\mathrm{SU}(3)_c$ as a triplet, under $\mathrm{SU}(2)_L$ as a doublet, and also carries nonzero

hypercharge: $\tilde{R}_2\,(\mathbf{3},\,\mathbf{2},\,1/6)$. The relevant couplings to fermions can be written as

$$\mathcal{L}_{\mathrm{LQs}} = \left[\bar{Q}_L^{ci} y^{LL} \epsilon^{ij} L_L^j + \bar{d}_R^c y^{\overline{RR}} \nu_R \right] S_1$$
$$+ \left[\bar{Q}_L^i y^{\overline{LR}} \nu_R - \bar{d}_R \epsilon^{ij} y^{RL} L_L^j \right] \tilde{R}^i + \mathrm{h.c.}\,, \tag{5.1}$$

where $y^{LL,RL}$ and $y^{\overline{RR},\overline{LR}}$ are 3×3 and $3\times n$ Yukawa matrices, respectively, while i,j are $\mathrm{SU}(2)_L$ indices. Integrating out the two LQs at tree level gives rise to dim-6 operators and at low energies the effective interactions between neutrinos and the first-generation quarks and charged-leptons become

$$\mathcal{L}^{(6)} \supset \frac{2G_F}{\sqrt{2}} \left[c_{\mathrm{VL}}^{(6)}(\bar{u}_L \gamma^\mu d_L)(\bar{e}_L \gamma_\mu \nu_{L\,\alpha}) + \bar{c}_{\mathrm{SR}}^{(6)}(\bar{u}_L d_R)(\bar{e}_L \nu_{R\,a}) + \bar{c}_{\mathrm{T}}^{(6)}(\bar{u}_L \sigma^{\mu\nu} d_R)(\bar{e}_L \sigma^{\mu\nu} \nu_{R\,a}) \right], \tag{5.2}$$

where we neglected neutral-current operators that are not relevant for single- and double-β decays. Furthermore, $\alpha = 1,\ldots 3$ and $a = 1,\ldots n$ indicate the active and sterile neutrinos and the Wilson coefficients are given by

$$c_{\mathrm{VL}}^{(6)} = -2V_{ud}\delta_{e\alpha} - \frac{v^2}{2M_1^2} y_{1e}^{LL*} y_{1\alpha}^{LL}\,,$$

$$\bar{c}_{\mathrm{SR}}^{(6)} = \frac{v^2}{2} \left(\frac{y_{1a}^{\overline{LR}} y_{1e}^{RL*}}{M_2^2} - \frac{y_{1a}^{\overline{RR}} y_{1e}^{LL*}}{M_1^2} \right),$$

$$\bar{c}_{\mathrm{T}}^{(6)} = \frac{v^2}{8} \left(\frac{y_{1a}^{\overline{LR}} y_{1e}^{RL*}}{M_2^2} + \frac{y_{1a}^{\overline{RR}} y_{1e}^{LL*}}{M_1^2} \right). \tag{5.3}$$

In the mass basis the matching coefficients become

$$\left(C_{\mathrm{VLL}}^{(6)} \right)_{ei} = \sum_{\alpha=1}^{3} c_{\mathrm{VL}\,e\alpha}^{(6)} U_{\alpha i}\,,$$

$$\left(C_{\mathrm{SRR}}^{(6)} \right)_{ei} = \sum_{a=1}^{n} \bar{c}_{\mathrm{SR}\,ea}^{(6)} U_{3+a,i}^*\,,$$

$$\left(C_{\mathrm{TRR}}^{(6)} \right)_{ei} = \sum_{a=1}^{n} \bar{c}_{\mathrm{T}\,ea}^{(6)} U_{3+a,i}^*\,. \tag{5.4}$$

A simplification is made possible by the fact that, as pointed out in ref. [5], the Wilson coefficient $C_{\mathrm{VLL}}^{(6)}$ cannot be independently determined by the nuclear data alone. In particularly, in eq. (2.11), it is *not* possible to distinguish the pure CKM element V_{ud} from the new physics contamination parameterized by $V_{ud}(1 + \epsilon_L + \epsilon_R)$.[9] We therefore absorb $C_{\mathrm{VLL}}^{(6)}$ into the CKM element V_{ud}, and only consider two Wilson coefficients $C_{\mathrm{SRR}}^{(6)}$ and $C_{\mathrm{TRR}}^{(6)}$ in this simple LQ model.

---

[9]The data only constrain four Wilson coefficients $C_{V,A,S,T}^+$, which depend on five parameters: V_{ud} and $\epsilon_{L,R,S,T}$, leaving one flat direction.
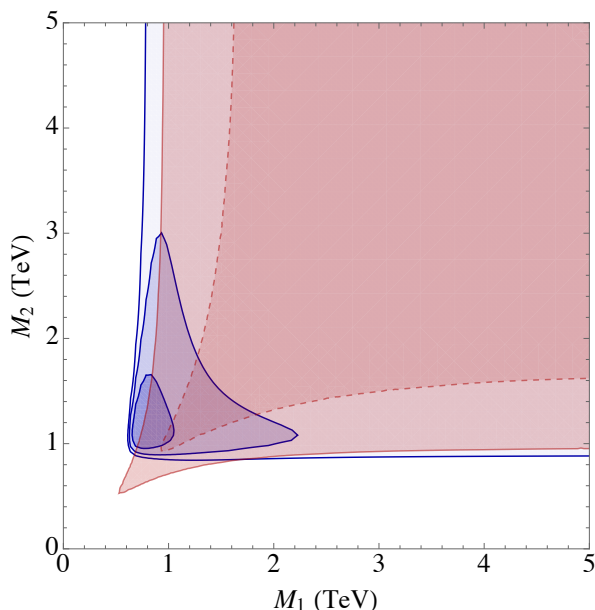
Figure 5. The red (dashed) line shows the current (future) limit from $0\nu\beta\beta$ for $m_{\nu_R} = 10\,\text{eV}$. The blue regions denote the $\Delta\chi^2 = 1, 2, 3$ contours from the single-β decay fit.

We show the resulting allowed regions in the $M_1 - M_2$ plane in figure 5, where we set $y_{11}^{\overline{LR}} y_{1e}^{RL*} = y_{11}^{\overline{RR}} y_{1e}^{LL*} = 1$ for simplicity. Here the red (dashed) contours show the (future) $0\nu\beta\beta$ limits for $m_4 = 10\,\text{eV}$, while the blue regions denote the $\Delta\chi^2 = 1, 2, 3$ contours from single-β decays. These $0\nu\beta\beta$ limits were obtained assuming there are no significant cancelations between the $\sim m_{\beta\beta}$ and non-standard contributions. In addition, we used the NMEs from ref. [52] and do not show the theoretical uncertainties due to the nuclear and hadronic matrix elements. The figure clearly shows the preference of the single-β fit for a nonzero tensor coupling, C_T^-, represented by the closed contours at $\Delta\chi^2 = 1, 2$, while for $\Delta\chi^2 = 3$ the fit allows for $C_T^- \to 0$ and for the LQ masses to decouple. By assuming that neutrinos are Majorana one can again compare to the current $0\nu\beta\beta$ limits. From the figure, one can see that these constraints are already cutting into the region preferred by single-β decay at $\Delta\chi^2 = 1$, for $m_{\nu_R} = 10\,\text{eV}$. The prospective EXO-200 measurements would allow one the completely exclude the $\Delta\chi^2 = 1$ region and large parts of the $\Delta\chi^2 = 2$ parameter space.

It should be mentioned that the considered scenario does not provide a complete description of neutrino masses or attempt to reconcile with direct collider observables which typically exclude LQs with masses below 1–2 TeV [60, 61]. A realistic model would therefore require more involved model building beyond the relatively simple extension of the SM considered here. We nevertheless consider the above scenario as a toy model as it clearly shows the complementary information on the nature and size of neutrino masses $0\nu\beta\beta$ could provide once a signal of nonzero BSM couplings would be found in probes of single β.

6   Conclusions

Sterile neutrinos play a role in numerous promising extensions of the SM and are strongly motivated by the necessity to generate neutrino masses. If sterile neutrinos exist, it is very possible that neutrinos are Majorana particles as no SM symmetries forbid sterile Majorana masses. In broad classes of SM extensions, sterile neutrinos only appear sterile at low energies, but interact through the exchange of heavy beyond-the-Standard-Model particles. Such SM extensions include left-right symmetric models, GUTs, leptoquark, and Z' models. In this work we studied how such interactions can be probed in β- and $0\nu\beta\beta$-decay experiments and in particular how these experiments complement each other in determining the mass and nature, Dirac or Majorana, of neutrinos.

To do so we employed the analysis of ref. [8] which performed a comprehensive analysis of non-standard neutrino interactions in β-decay experiments. They demonstrated that precision β-decay experiments probe non-standard couplings to sterile neutrinos at the $\mathcal{O}(10^{-1} - 10^{-2})$ level, corresponding to BSM scales of a few TeV. They also found a slight hint for a nonzero tensor coupling to sterile neutrinos. We addressed what these results imply for the search of sterile neutrinos with $0\nu\beta\beta$ decay experiments. On the $0\nu\beta\beta$ side, we calculated the decay rates as a function of sterile neutrino masses and non-standard couplings at the dimension-six level of the neutrino-extended Standard Model Effective Field Theory. We focussed on rather light sterile neutrinos as only these can be produced in neutron and nuclear β-decay processes. It is worthwhile to mention that the KATRIN experiment, which measures the tritium β-decay spectrum, may also provide competitive constraints on the non-standard couplings of the sterile neutrino within our mass range. Given the current limits, the non-standard couplings could induce relative distortions of the spectrum at the per mille level [62]. As was shown for a benchmark calculation with $m_{\nu_R} \sim 5\,\mathrm{keV}$, these effects could allow for improved constraints assuming that the whole electron energy spectrum of KATRIN is accessible and theoretical and systematical uncertainties can be reduced below the per mille level.

For sufficiently small masses, β-decay constraints are neutrino-mass independent whereas $0\nu\beta\beta$ decay rates scale quadratically with the Majorana mass. We showed that, barring cancelations between $\sim m_{\beta\beta}$ and non-standard contributions, $0\nu\beta\beta$ measurements start to become competitive for right-handed neutrino masses larger than about $100\,\mathrm{eV}$ with a mild dependence on the particular interaction under consideration. Under the same assumptions, we also discussed the range of neutrino masses for which one would expect a measurable signal in $0\nu\beta\beta$, assuming couplings of right-handed neutrinos were to be confirmed in either single β decays or at the LHC. For right-handed neutrino couplings of the size indicated by the hint in the recent β-decay results, we show that next-generation $0\nu\beta\beta$ experiments would be able to determine the Dirac or Majorana nature of neutrinos for $m_{\nu_R} \gtrsim 3\,\mathrm{eV}$. Finally, we discussed the implications of the hints in single-β and the $0\nu\beta\beta$ limits in the context of a specific (toy) model of BSM physics involving two leptoquarks. Such a model with TeV leptoquark masses can account for the discrepancy and imply a measurable signal in next-generation $0\nu\beta\beta$ experiments unless neutrinos are Dirac particles.

Our study demonstrates the complementary nature of different neutrino probes, and the various aspects of the theory space they individually are sensitive to. In case of a

future discovery of a deviation from the Standard Model predictions in one of the experiments, looking at other probes in a global approach provides valuable information to better understand the nature of neutrinos.

Acknowledgments

A νSMEFT operators and matching

Here we briefly discuss the dimension-six operators making up the νSMEFT Lagrangian in eq. (2.1) and give the matching of these operators onto the low-energy Lagrangian of eq. (2.9). The dimension-six Lagrangian involving left- and right-handed neutrinos, $\mathcal{L}_{\nu_{L,R}}^{(\bar{6})}$, is given by the sum of the operators (and their hermitian conjugates) in table 3 and table 4, respectively, where each operator is multiplied by a corresponding Wilson coefficient. The matching contributions of these Wilson coefficients to the couplings to left-handed neutrinos can then be written as,

$$
\begin{aligned}
C_{\mathrm{VLL}}^{(6)} &= \left[-2V_{ud}\mathbb{1} + 2v^2 \left[C_{LQ\,3}^{(6)} - C_{HL\,3}^{(6)} - C_{HQ\,3}^{(6)}\mathbb{1} \right] - \frac{4\sqrt{2}v}{g} M_e \left(C_{eW}^{(6)} \right)^\dagger \right. \\
&\quad \left. - \frac{4\sqrt{2}v}{g} C_{\nu W}^{(6)} M_D^\dagger \right] PU - \frac{4\sqrt{2}v}{g} C_{\nu W}^{(6)} M_R^\dagger P_s U \,, \\
C_{\mathrm{VRL}}^{(6)} &= -v^2 C_{Hud}^{(6)} PU, \\
C_{\mathrm{SRL}}^{(6)} &= v^2 \left(C_{LedQ}^{(6)} \right)^\dagger PU \,, \\
C_{\mathrm{SLL}}^{(6)} &= v^2 \left(C_{LeQu\,1}^{(6)} \right)^\dagger PU \,, \\
C_{\mathrm{TLL}}^{(6)} &= v^2 \left(C_{LeQu\,3}^{(6)} \right)^\dagger PU \,,
\end{aligned}
\tag{A.1}
$$

where the first contribution to $C_{\mathrm{VLL}}^{(6)}$ is the SM contribution.

The Wilson coefficient of the operators involving right-handed chiralities are,

$$
\begin{aligned}
C_{\mathrm{VLR}}^{(6)} &= \left[-v^2 C_{H\nu e}^{(6)} - \frac{4\sqrt{2}v}{g} \left(C_{\nu W}^{(6)} \right)^\dagger M_e - \frac{4\sqrt{2}v}{g} M_D^\dagger C_{eW}^{(6)} \right]^\dagger P_s U^* \,, \\
C_{\mathrm{VRR}}^{(6)} &= v^2 \left(C_{du\nu e}^{(6)} \right)^\dagger P_s U^* \,, \\
C_{\mathrm{SRR}}^{(6)} &= \left[-v^2 C_{L\nu Qd}^{(6)} + \frac{v^2}{2} C_{LdQ\nu}^{(6)} \right] P_s U^* \,, \\
C_{\mathrm{SLR}}^{(6)} &= v^2 \left(C_{Qu\nu L}^{(6)} \right)^\dagger P_s U^* \,, \\
C_{\mathrm{TRR}}^{(6)} &= \frac{v^2}{8} C_{LdQ\nu}^{(6)} P_s U^* \,.
\end{aligned}
\tag{A.2}
$$

Class 1	$\psi^2 H X$	Class 2	$\psi^2 H^2 D$	Class 3	ψ^4
$\mathcal{O}_{eW}^{(6)}$	$(\bar{L}\sigma^{\mu\nu}e)\tau^I H W_{\mu\nu}^I$	$\mathcal{O}_{HL3}^{(6)}$	$(H^\dagger i\overleftrightarrow{D}_\mu^I H)(\bar{L}\tau^I\gamma^\mu L)$	$\mathcal{O}_{LeQu1}^{(6)}$	$(\bar{L}^j e)\epsilon_{jk}(\bar{Q}^k u)$
$\mathcal{O}_{uW}^{(6)}$	$(\bar{Q}\sigma^{\mu\nu}u)\tau^I \widetilde{H} W_{\mu\nu}^I$	$\mathcal{O}_{HQ3}^{(6)}$	$(H^\dagger i\overleftrightarrow{D}_\mu^I H)(\bar{Q}\tau^I\gamma^\mu Q)$	$\mathcal{O}_{LeQu3}^{(6)}$	$(\bar{L}^j \sigma_{\mu\nu}e)\epsilon_{jk}(\bar{Q}^k\sigma^{\mu\nu}u)$
$\mathcal{O}_{dW}^{(6)}$	$(\bar{Q}\sigma^{\mu\nu}d)\tau^I H W_{\mu\nu}^I$	$\mathcal{O}_{Hud}^{(6)}$	$i(\widetilde{H}^\dagger D_\mu H)(\bar{u}\gamma^\mu d)$	$\mathcal{O}_{LQ3}^{(6)}$	$(\bar{L}\gamma^\mu\tau^I L)(\bar{Q}\gamma_\mu\tau^I Q)$
				$\mathcal{O}_{LedQ}^{(6)}$	$(\bar{L}^j e)(\bar{d}Q^j)$

Table 3. LNC dim-6 operators [63] involving active neutrinos that affect $0\nu\beta\beta$ at tree level.

Class 1	$\psi^2 H^3$	Class 4	ψ^4
$\mathcal{O}_{L\nu H}^{(6)}$	$(\bar{L}\nu_R)\tilde{H}(H^\dagger H)$	$\mathcal{O}_{du\nu e}^{(6)}$	$(\bar{d}\gamma^\mu u)(\bar{\nu}_R\gamma_\mu e)$
Class 2	$\psi^2 H^2 D$	$\mathcal{O}_{Qu\nu L}^{(6)}$	$(\bar{Q}u)(\bar{\nu}_R L)$
$\mathcal{O}_{H\nu e}^{(6)}$	$(\bar{\nu}_R\gamma^\mu e)(\tilde{H}^\dagger i D_\mu H)$	$\mathcal{O}_{L\nu Qd}^{(6)}$	$(\bar{L}\nu_R)\epsilon(\bar{Q}d))$
Class 3	$\psi^2 H^3 D$	$\mathcal{O}_{LdQ\nu}^{(6)}$	$(\bar{L}d)\epsilon(\bar{Q}\nu_R)$
$\mathcal{O}_{\nu W}^{(6)}$	$(\bar{L}\sigma_{\mu\nu}\nu_R)\tau^I \tilde{H} W^{I\mu\nu}$		

Table 4. LNC dim-6 operators [64] involving a sterile neutrino that affect $0\nu\beta\beta$ at tree level.

B Details of the $0\nu\beta\beta$ calculation

Here we briefly discuss the ingredients involved in the calculation of $0\nu\beta\beta$ decay rates that were not fully explained in section 3.2. We start with the definition of the nuclear matrix elements (NMEs), after which we discuss the subamplitudes, $\mathcal{A}_{L,R,M}^{(\nu)}(m_i)$, that are induced by the exchange of hard neutrinos.

B.1 Nuclear matrix elements

The NMEs used in section 3.2 are defined as follows,

$$\mathcal{M}_V(m_i) = -\frac{g_V^2}{g_A^2}M_F(m_i) + M_{GT}^{MM}(m_i) + M_T^{MM}(m_i),$$

$$\mathcal{M}_A(m_i) = M_{GT}^{AA}(m_i) + M_{GT}^{AP}(m_i) + M_{GT}^{PP}(m_i) + M_T^{AP}(m_i) + M_T^{PP}(m_i),$$

$$\mathcal{M}_{PS}(m_i) = \frac{1}{2}M_{GT}^{AP}(m_i) + M_{GT}^{PP}(m_i) + \frac{1}{2}M_T^{AP}(m_i) + M_T^{PP}(m_i),$$

$$\mathcal{M}_{PS,sd} = \frac{1}{2}M_{GT,sd}^{AP}(0) + M_{GT,sd}^{PP}(0) + \frac{1}{2}M_{T,sd}^{AP}(0) + M_{T,sd}^{PP}(0),$$

$$\mathcal{M}_S(m_i) = \frac{g_S^2}{g_A^2}M_F(m_i),$$

$$\mathcal{M}_T(m_i) = 16\frac{g_T^2}{g_A^2}M_{GT}^{AA}(m_i),$$

$$\mathcal{M}_{TV}(m_i) = -4\frac{g_T' g_V}{g_A^2}\frac{m_\pi^2}{m_N^2}M_{F,sd}(m_i) + \frac{16g_T}{g_M}\left[M_{GT}^{MM}(m_i) + M_T^{MM}(m_i)\right],$$

$$\mathcal{M}_{VA}(m_i) = 2\frac{g_A}{g_M}\left[M_{GT}^{MM}(m_i) + M_T^{MM}(m_i)\right],$$

$$\mathcal{M}_{TA}(m_i) = \frac{g_T}{g_A}\left[2M_{GT}^{AA}(m_i) + M_{GT}^{AP}(m_i) + M_T^{AP}(m_i)\right], \tag{B.1}$$

NMEs	^{76}Ge			^{82}Se		^{130}Te		^{136}Xe	
	[52]	[51]	[66, 67]	[52]	[51]	[52]	[51]	[52]	[51]
M_F	-1.74	-0.59	-0.68	-1.29	-0.55	-1.52	-0.67	-0.89	-0.54
M_{GT}^{AA}	5.48	3.15	5.06	3.87	2.97	4.28	2.97	3.16	2.45
M_{GT}^{AP}	-2.02	-0.94	-0.92	-1.46	-0.89	-1.74	-0.97	-1.19	-0.79
M_{GT}^{PP}	0.66	0.30	0.24	0.48	0.28	0.59	0.31	0.39	0.25
M_{GT}^{MM}	0.51	0.22	0.17	0.37	0.20	0.45	0.23	0.31	0.19
M_T^{AA}	—	—	—	—	—	—	—	—	—
M_T^{AP}	-0.35	-0.01	-0.31	-0.27	-0.01	-0.50	0.01	-0.28	0.01
M_T^{PP}	0.10	0.00	0.09	0.08	0.00	0.16	-0.01	0.09	-0.01
M_T^{MM}	-0.04	0.00	-0.04	-0.03	0.00	-0.06	0.00	-0.03	0.00
$M_{F,sd}$	-3.46	-1.46	-1.1	-2.53	-1.37	-2.97	-1.61	-1.53	-1.28
$M_{GT,sd}^{AA}$	11.1	4.87	3.62	7.98	4.54	10.1	5.31	5.71	4.25
$M_{GT,sd}^{AP}$	-5.35	-2.26	-1.37	-3.82	-2.09	-4.94	-2.51	-2.80	-1.99
$M_{GT,sd}^{PP}$	1.99	0.82	0.42	1.42	0.77	1.86	0.92	1.06	0.74
$M_{T,sd}^{AP}$	-0.85	-0.05	-0.97	-0.65	-0.05	-1.50	0.07	-0.92	0.05
$M_{T,sd}^{PP}$	0.32	0.02	0.38	0.24	0.02	0.58	-0.02	0.36	-0.02

Table 5. Comparison of NMEs computed in the quasi-particle random phase approximation [52], shell model [51], and interacting boson model [66, 67] for several isotopes of experimental interest. See e.g. [68] for a more recent calculation in the interacting boson model which, however, uses slightly differently defined matrix elements.

in terms of a set of NMEs and the low-energy constants $g_T = 0.99 \pm 0.03$, $g_M = 4.7$, and the unknown $g_T' = \mathcal{O}(1)$ which we set to 1 in this work. The small m_i limits of the NMEs have been calculated in the literature. We show the numerical values of $M_K^a(0)$ and $M_{K,sd}^a(0)$, with $K = F, GT, T$ and $a = AA, AP, PP, MM$, for several calculations and different isotopes in table 5.

To obtain the m_i dependence of these matrix elements we follow refs. [23, 65] and interpolate between the low- and high-mass regimes, where the relevant matrix elements are available. This is possible since $M_K^a(0)$ have been determined in the literature, while the large-mass limits are in most cases are related to the short-distance matrix elements, $M_{K,sd}^a(0)$. For example, for the Fermi matrix element we use

$$M_{F\,\text{int}}(m_i) = M_{F,sd}\frac{m_\pi^2}{m_i^2 + m_\pi^2 \frac{M_{F,sd}}{M_F}}\,, \tag{B.2}$$

which has the correct $m_i \to 0$ and $m_i \to \infty$ behavior. We construct analogous expressions for $M_{GT,T\,\text{int}}^{AA}(m_i)$, $M_{GT,T\,\text{int}}^{AP}(m_i)$, and $M_{GT,T\,\text{int}}^{PP}(m_i)$. The m_i dependence of the remaining matrix elements in table 5 can be related to the previously discussed NMEs. For the

magnetic GT matrix element we have,

$$M_{GT}^{MM}(m_i) = \frac{g_M^2}{6g_A^2}\left[\frac{m_\pi^2}{m_N^2}M_{GT,\,sd}^{AA} - \frac{m_i^2}{m_N^2}M_{GT}^{AA}(m_i)\right],\tag{B.3}$$

and the for short-distance NMEs

$$M_{F,\,sd}(m_i) = M_{F,\,sd} - \frac{m_i^2}{m_\pi^2}M_F(m_i)\,,$$

$$M_{GT,\,sd}^{ab}(m_i) = M_{GT,\,sd}^{ab} - \frac{m_i^2}{m_\pi^2}M_{GT}^{ab}(m_i)\,,$$

$$M_{T,\,sd}^{ab}(m_i) = M_{T,\,sd}^{ab} - \frac{m_i^2}{m_\pi^2}M_T^{ab}(m_i)\,.\tag{B.4}$$

B.2 Hard neutrino exchange

The contributions due to hard neutrinos can be written as,

$$\mathcal{A}_L^{(\nu)}(m_i) = \frac{m_\pi^2}{m_e v}\left[\left(\frac{C_{iL}^{\pi\pi}}{m_\pi^2} + C_{iL}'^{\pi\pi}\right)\mathcal{M}_{PS,sd} + \frac{C_{iL}^{\pi N} - C_{iL}'^{\pi\pi}}{2}\left(M_{GT,\,sd}^{AP} + M_{T,\,sd}^{AP}\right)\right.$$

$$\left. - \frac{2}{g_A^2}C_{iL}^{NN}M_{F,\,sd}\right],$$

$$\mathcal{A}_M^{(\nu)} = \frac{m_\pi^2}{m_e v}\left[-\frac{2}{g_A^2}C_{iV}^{NN}M_{F,\,sd} + \frac{1}{2}C_{iV}^{\pi N}\left(M_{GT,\,sd}^{AP} + M_{T,\,sd}^{AP}\right)\right],\tag{B.5}$$

in terms of the effective $\pi\pi$, πN, and NN interactions, $C_i^{\pi\pi}$, $C_i^{\pi N}$, and C_i^{NN}. $\mathcal{A}_R^{(\nu)}(m_i)$ can be obtained by replacing $C_{iL}^\alpha \to C_{iR}^\alpha$. In the case of the dimension-six couplings under consideration here, together with the approximation in which we drop the interference terms with the SM weak current as discussed in section 3.2, several of the above terms vanish. It turns out that the derivative pion terms as well as the pion-nucleon couplings go to zero with the above approximations, so that we have $C_{iL}'^{\pi\pi} = C_{iL}^{\pi N} = C_{iV}^{\pi N} = 0$. The remaining $C_\alpha^{\pi\pi}$ couplings are given by,

$$C_{iL,R}^{\pi\pi} = \frac{m_i v}{F_\pi^2}c_{iL,R}^{\nu\pi\pi}\,,$$

$$c_{iL}^{\nu\pi\pi} = 2g_{LR}^{\pi\pi}(m_i)\left(C_{VLL}^{(6)}\right)_{ei}\left(C_{VRL}^{(6)}\right)_{ei} - 2g_{S1}^{\pi\pi}(m_i)\left[\left(C_{SLR}^{(6)}\right)_{ei}^2 + \left(C_{SRR}^{(6)}\right)_{ei}^2\right]$$

$$+ 4g_{S2}^{\pi\pi}(m_i)\left(C_{SLR}^{(6)}\right)_{ei}\left(C_{SRR}^{(6)}\right)_{ei} - 2g_{TT}^{\pi\pi}(m_i)\left(C_{TRR}^{(6)}\right)_{ei}^2\,.\tag{B.6}$$

Here, all LECs scale as $g_i^{\pi\pi} = \mathcal{O}(F_\pi^2)$ and the right-handed coupling $c_{iR}^{\nu\pi\pi}$ can be obtained from $c_{iL}^{\nu\pi\pi}$ by interchanging the L, R labels on the Wilson coefficients, $L \leftrightarrow R$, while leaving those on the LECs unchanged.

The relevant NN couplings can be written as,

$$C_{i\,L,R,V}^{\mathrm{NN}} = \frac{m_i}{\Lambda_\chi} c_{i\,L,R,V}^{\nu\mathrm{NN}} \,,$$

$$\begin{aligned}
\frac{c_{i\,L}^{\nu\mathrm{NN}}}{v\Lambda_\chi} &= \frac{g_\nu^{\mathrm{NN}}(m_i)}{4} \left[\left(C_{\mathrm{VLL}}^{(6)}\right)_{ei}^2 + \left(C_{\mathrm{VRL}}^{(6)}\right)_{ei}^2 \right] + \frac{g_{\mathrm{LR}}^{\mathrm{NN}}(m_i)}{2} \left(C_{\mathrm{VLL}}^{(6)}\right)_{ei} \left(C_{\mathrm{VRL}}^{(6)}\right)_{ei} \\
&\quad + \frac{g_{\mathrm{S1}}^{\mathrm{NN}}(m_i)}{4} \left[\left(C_{\mathrm{SRR}}^{(6)}\right)_{ei}^2 + \left(C_{\mathrm{SLR}}^{(6)}\right)_{ei}^2 \right] - \frac{g_{\mathrm{S2}}^{\mathrm{NN}}(m_i)}{2} \left(C_{\mathrm{SRR}}^{(6)}\right)_{ei} \left(C_{\mathrm{SLR}}^{(6)}\right)_{ei} \\
&\quad + \frac{g_{\mathrm{TT}}^{\mathrm{NN}}(m_i)}{4} \left(C_{\mathrm{TRR}}^{(6)}\right)_{ei}^2 \,, \\
\frac{c_{i\,V}^{\nu\mathrm{NN}}}{v\Lambda_\chi} &= g_{\mathrm{SLL,VLL}}^{\mathrm{NN}}(m_i) \left[\left(C_{\mathrm{SLL}}^{(6)} + C_{\mathrm{SRL}}^{(6)}\right)_{ei} \left(C_{\mathrm{VLL}}^{(6)} + C_{\mathrm{VRL}}^{(6)}\right)_{ei} - (L \leftrightarrow R) \right] \\
&\quad + g_{\mathrm{TLL,VLL}}^{\mathrm{NN}}(m_i) \left[\left(C_{\mathrm{TLL}}^{(6)}\right)_{ei} \left(C_{\mathrm{VLL}}^{(6)} - C_{\mathrm{VRL}}^{(6)}\right)_{ei} - (L \leftrightarrow R) \right] \,.
\end{aligned} \tag{B.7}$$

The right-handed couplings $c_{i\,R}^{\mathrm{NN},\nu\mathrm{NN}}$ can again be obtained from $c_{i\,L}^{\mathrm{NN},\nu\mathrm{NN}}$ by interchanging the L, R labels on the Wilson coefficients, $L \leftrightarrow R$, while leaving those on the LECs unchanged. Note that some of the terms in eqs. (B.5) and (B.7) can be neglected given our assumptions, but can play a role in the right-handed couplings after the above replacement. Using naive-dimensional analysis would lead one to suspect that the g_α^{NN} scale as $1/\Lambda_\chi^2$, where $\Lambda_\chi \sim 1\,\mathrm{GeV}$ is the breakdown scale of chiral perturbation theory. However, it turns out that these LECs need to be enhanced by Λ_χ^2/F_π^2 in order to obtain renormalized amplitudes, so that $g_\alpha^{NN} \sim 1/F_\pi^2$, see ref. [23] for more details.

Similar to the m_i dependence of the NMEs, we use the low- and high-mass limits of the LECs to construct interpolation formulae for these hadronic matrix elements. The interpolation we use is of the form

$$g_\alpha(m_i)\big|_{\mathrm{naive}} = \frac{g_\alpha(0)}{1 + g_\alpha(0) \left[\frac{m_0^2}{m_i^2} \bar{g}_\alpha(m_0)\right]^{-1}} \,, \tag{B.8}$$

where $m_0 \simeq 2\,\mathrm{GeV}$ is a scale at which the procedure of integrating out the heavy neutrino becomes reliable. The $\bar{g}_\alpha(m)$ are effective LECs, scaling as $1/m^2$, which are needed in the $m_i \geq m_0$ region to ensure the amplitude reproduces the result from integrating out the neutrino at the quark level. The above expression reduces to $g_\alpha(0)$ for $m_i \ll m_\pi$ and $\frac{m_0^2}{m_i^2} \bar{g}_\alpha(m_0)$ for $m_i \to \infty$. The required input to these interpolation formulae are thus $g_\alpha(0)$ and $\bar{g}_\alpha(m_i)$, where the latter depends on the matrix elements of the dimension-nine operators, $\sim (\bar{u}d)^2 \bar{e}e^c$, that arise after integrating out neutrinos at the quark level. For simplicity we neglect the QCD evolution of these matrix elements, which can in principle be captured by eq. (B.8).

Performing the matching to the amplitudes that result from integrating out neutrinos with $m_i \gtrsim 2\,\mathrm{GeV}$ gives rise to the following expressions for the $\pi\pi$ LECs

$$\begin{aligned}
g_{\mathrm{LR}}^{\pi\pi}(m_i) &= g_{\mathrm{LR}}^{\pi\pi}(0) \frac{1}{1 - 4\frac{m_i^2}{F_\pi^2} g_{\mathrm{LR}}^{\pi\pi}(0) \left[g_4^{\pi\pi}(m_0)\right]^{-1}} \,, \\
g_{\mathrm{S1}}^{\pi\pi}(m_i) &= g_{\mathrm{S1}}^{\pi\pi}(0) \frac{1}{1 + 8\frac{m_i^2}{F_\pi^2} g_{\mathrm{S1}}^{\pi\pi}(0) \left[g_2^{\pi\pi}(m_0) - B^2\right]^{-1}} \,,
\end{aligned}$$

$$g_{\text{S2}}^{\pi\pi}(m_i) = g_{\text{S2}}^{\pi\pi}(0) \frac{1}{1 - 8\frac{m_i^2}{F_\pi^2} g_{\text{S2}}^{\pi\pi}(0) \left[g_5^{\pi\pi}(m_0)/2 - B^2\right]^{-1}},$$

$$g_{\text{TT}}^{\pi\pi}(m_i) = g_{\text{TT}}^{\pi\pi}(0) \frac{1}{1 + \frac{m_i^2}{F_\pi^2} g_{\text{TT}}^{\pi\pi}(0) \left[4g_3^{\pi\pi}(m_0) + 2g_2^{\pi\pi}(m_0)\right]^{-1}}. \tag{B.9}$$

Similar expressions can in principle be derived for the NN LECs [23], currently, however, none of the needed LECs are known in the NN sector. The techniques of refs. [69, 70] where the short-distance LECs for the LL case were calculated can in principle be applied to non-standard interactions as well, but this has not been done so far. In our numerical analysis we therefore estimate the hard-neutrino contributions by considering the $\pi\pi$ terms, while neglecting the NN pieces. We take the following values for the needed LECs,

$$g_{\text{LR}}^{\pi\pi}(0) = g_{\text{TT}}^{\pi\pi}(0) = -g_{\text{S1}}^{\pi\pi}(0) = -g_{\text{S2}}^{\pi\pi}(0) = F_\pi^2, \qquad g_\alpha^{NN}(0) = 0,$$

$$g_2^{\pi\pi} = 2.0\,\text{GeV}^2, \qquad g_3^{\pi\pi} = -0.62\,\text{GeV}^2,$$

$$g_4^{\pi\pi} = -1.9\,\text{GeV}^2, \qquad g_5^{\pi\pi} = -8.0\,\text{GeV}^2. \tag{B.10}$$

Here the values for $g_\alpha^{\pi\pi}(0)$ are consistent with NDA estimates, while we use the lattice QCD results of ref. [49] for $g_{2,3,4,5}^{\pi\pi}$ evaluated at $\mu = 2\,\text{GeV}$.

Open Access. This article is distributed under the terms of the Creative Commons Attribution License ([CC-BY 4.0](#)), which permits any use, distribution and reproduction in any medium, provided the original author(s) and source are credited.

References

[1] T.D. Lee and C.-N. Yang, *Question of Parity Conservation in Weak Interactions*, [*Phys. Rev.* **104** (1956) 254](#) [INSPIRE].

[2] O. Naviliat-Cuncic and M. González-Alonso, *Prospects for precision measurements in nuclear β decay at the LHC era*, [*Annalen Phys.* **525** (2013) 600](#) [arXiv:1304.1759] [INSPIRE].

[3] V. Cirigliano, S. Gardner and B. Holstein, *Beta Decays and Non-Standard Interactions in the LHC Era*, [*Prog. Part. Nucl. Phys.* **71** (2013) 93](#) [arXiv:1303.6953] [INSPIRE].

[4] K.K. Vos, H.W. Wilschut and R.G.E. Timmermans, *Symmetry violations in nuclear and neutron β decay*, [*Rev. Mod. Phys.* **87** (2015) 1483](#) [arXiv:1509.04007] [INSPIRE].

[5] M. González-Alonso, O. Naviliat-Cuncic and N. Severijns, *New physics searches in nuclear and neutron β decay*, [*Prog. Part. Nucl. Phys.* **104** (2019) 165](#) [arXiv:1803.08732] [INSPIRE].

[6] I. Bischer and W. Rodejohann, *General neutrino interactions from an effective field theory perspective*, [*Nucl. Phys. B* **947** (2019) 114746](#) [arXiv:1905.08699] [INSPIRE].

[7] J.C. Hardy and I.S. Towner, *Superallowed $0^+ \to 0^+$ nuclear β decays: 2020 critical survey, with implications for V_{ud} and CKM unitarity*, [*Phys. Rev. C* **102** (2020) 045501](#) [INSPIRE].

[8] A. Falkowski, M. González-Alonso and O. Naviliat-Cuncic, *Comprehensive analysis of beta decays within and beyond the Standard Model*, [*JHEP* **04** (2021) 126](#) [arXiv:2010.13797] [INSPIRE].

[9] M. Beck et al., *Improved determination of the β-$\overline{\nu}_e$ angular correlation coefficient a in free neutron decay with the aSPECT spectrometer*, *Phys. Rev. C* **101** (2020) 055506 [arXiv:1908.04785] [INSPIRE].

[10] Y. Grossman, E. Passemar and S. Schacht, *On the Statistical Treatment of the Cabibbo Angle Anomaly*, *JHEP* **07** (2020) 068 [arXiv:1911.07821] [INSPIRE].

[11] A. Crivellin, F. Kirk, C.A. Manzari and M. Montull, *Global Electroweak Fit and Vector-Like Leptons in Light of the Cabibbo Angle Anomaly*, *JHEP* **12** (2020) 166 [arXiv:2008.01113] [INSPIRE].

[12] A. Crivellin and M. Hoferichter, *β Decays as Sensitive Probes of Lepton Flavor Universality*, *Phys. Rev. Lett.* **125** (2020) 111801 [arXiv:2002.07184] [INSPIRE].

[13] A. Crivellin, M. Hoferichter and C.A. Manzari, *Fermi Constant from Muon Decay Versus Electroweak Fits and Cabibbo-Kobayashi-Maskawa Unitarity*, *Phys. Rev. Lett.* **127** (2021) 071801 [arXiv:2102.02825] [INSPIRE].

[14] J.C. Pati and A. Salam, *Lepton Number as the Fourth Color*, *Phys. Rev. D* **10** (1974) 275 [*Erratum ibid.* **11** (1975) 703] [INSPIRE].

[15] R.N. Mohapatra and J.C. Pati, *Left-Right Gauge Symmetry and an Isoconjugate Model of CP-violation*, *Phys. Rev. D* **11** (1975) 566 [INSPIRE].

[16] G. Senjanović and R.N. Mohapatra, *Exact Left-Right Symmetry and Spontaneous Violation of Parity*, *Phys. Rev. D* **12** (1975) 1502 [INSPIRE].

[17] M. Drewes et al., *A White Paper on keV Sterile Neutrino Dark Matter*, *JCAP* **01** (2017) 025 [arXiv:1602.04816] [INSPIRE].

[18] P.D. Bolton, F.F. Deppisch and P.S. Bhupal Dev, *Neutrinoless double beta decay versus other probes of heavy sterile neutrinos*, *JHEP* **03** (2020) 170 [arXiv:1912.03058] [INSPIRE].

[19] A. Boyarsky, O. Ruchayskiy and M. Shaposhnikov, *The Role of sterile neutrinos in cosmology and astrophysics*, *Ann. Rev. Nucl. Part. Sci.* **59** (2009) 191 [arXiv:0901.0011] [INSPIRE].

[20] O. Ruchayskiy and A. Ivashko, *Restrictions on the lifetime of sterile neutrinos from primordial nucleosynthesis*, *JCAP* **10** (2012) 014 [arXiv:1202.2841] [INSPIRE].

[21] A.C. Vincent, E.F. Martínez, P. Hernández, M. Lattanzi and O. Mena, *Revisiting cosmological bounds on sterile neutrinos*, *JCAP* **04** (2015) 006 [arXiv:1408.1956] [INSPIRE].

[22] M. Nemevšek, G. Senjanović and Y. Zhang, *Warm Dark Matter in Low Scale Left-Right Theory*, *JCAP* **07** (2012) 006 [arXiv:1205.0844] [INSPIRE].

[23] W. Dekens, J. de Vries, K. Fuyuto, E. Mereghetti and G. Zhou, *Sterile neutrinos and neutrinoless double beta decay in effective field theory*, *JHEP* **06** (2020) 097 [arXiv:2002.07182] [INSPIRE].

[24] V. Cirigliano, W. Dekens, J. de Vries, M.L. Graesser and E. Mereghetti, *Neutrinoless double beta decay in chiral effective field theory: lepton number violation at dimension seven*, *JHEP* **12** (2017) 082 [arXiv:1708.09390] [INSPIRE].

[25] R.E. Shrock, *New Tests For, and Bounds On, Neutrino Masses and Lepton Mixing*, *Phys. Lett. B* **96** (1980) 159 [INSPIRE].

[26] D.A. Bryman and R. Shrock, *Constraints on Sterile Neutrinos in the MeV to GeV Mass Range*, *Phys. Rev. D* **100** (2019) 073011 [arXiv:1909.11198] [INSPIRE].

[27] M. Ademollo and R. Gatto, *Nonrenormalization Theorem for the Strangeness Violating Vector Currents*, *Phys. Rev. Lett.* **13** (1964) 264 [INSPIRE].

[28] FLAVOUR LATTICE AVERAGING GROUP collaboration, *FLAG Review 2019: Flavour Lattice Averaging Group (FLAG)*, *Eur. Phys. J. C* **80** (2020) 113 [arXiv:1902.08191] [INSPIRE].

[29] C.C. Chang et al., *A per-cent-level determination of the nucleon axial coupling from quantum chromodynamics*, *Nature* **558** (2018) 91 [arXiv:1805.12130] [INSPIRE].

[30] R. Gupta, Y.-C. Jang, B. Yoon, H.-W. Lin, V. Cirigliano and T. Bhattacharya, *Isovector Charges of the Nucleon from 2+1+1-flavor Lattice QCD*, *Phys. Rev. D* **98** (2018) 034503 [arXiv:1806.09006] [INSPIRE].

[31] M. González-Alonso and J. Martin Camalich, *Isospin breaking in the nucleon mass and the sensitivity of β decays to new physics*, *Phys. Rev. Lett.* **112** (2014) 042501 [arXiv:1309.4434] [INSPIRE].

[32] C.-Y. Seng, M. Gorchtein, H.H. Patel and M.J. Ramsey-Musolf, *Reduced Hadronic Uncertainty in the Determination of V_{ud}*, *Phys. Rev. Lett.* **121** (2018) 241804 [arXiv:1807.10197] [INSPIRE].

[33] A. Czarnecki, W.J. Marciano and A. Sirlin, *Radiative Corrections to Neutron and Nuclear Beta Decays Revisited*, *Phys. Rev. D* **100** (2019) 073008 [arXiv:1907.06737] [INSPIRE].

[34] C.-Y. Seng, X. Feng, M. Gorchtein and L.-C. Jin, *Joint lattice QCD-dispersion theory analysis confirms the quark-mixing top-row unitarity deficit*, *Phys. Rev. D* **101** (2020) 111301 [arXiv:2003.11264] [INSPIRE].

[35] L. Hayen, *Standard model $\mathcal{O}(\alpha)$ renormalization of g_A and its impact on new physics searches*, *Phys. Rev. D* **103** (2021) 113001 [arXiv:2010.07262] [INSPIRE].

[36] J.D. Jackson, S.B. Treiman and H.W. Wyld, *Possible tests of time reversal invariance in Beta decay*, *Phys. Rev.* **106** (1957) 517 [INSPIRE].

[37] M. Ebel and G. Feldman, *Further remarks on Coulomb corrections in allowed beta transitions*, *Nucl. Phys.* **4** (1957) 213.

[38] B.R. Holstein, *Recoil Effects in Allowed beta Decay: The Elementary Particle Approach*, *Rev. Mod. Phys.* **46** (1974) 789 [*Erratum ibid.* **48** (1976) 673] [INSPIRE].

[39] L. Hayen, N. Severijns, K. Bodek, D. Rozpedzik and X. Mougeot, *High precision analytical description of the allowed β spectrum shape*, *Rev. Mod. Phys.* **90** (2018) 015008 [arXiv:1709.07530] [INSPIRE].

[40] L. Hayen and A.R. Young, *Consistent description of angular correlations in β decay for Beyond Standard Model physics searches*, arXiv:2009.11364 [INSPIRE].

[41] E. Holzschuh, L. Palermo, H. Stussi and P. Wenk, *The beta-spectrum of S-35 and search for the admixture of heavy neutrinos*, *Phys. Lett. B* **482** (2000) 1 [INSPIRE].

[42] A.S. Riis and S. Hannestad, *Detecting sterile neutrinos with KATRIN like experiments*, *JCAP* **02** (2011) 011 [arXiv:1008.1495] [INSPIRE].

[43] C. Giunti, Y.F. Li and Y.Y. Zhang, *KATRIN bound on 3+1 active-sterile neutrino mixing and the reactor antineutrino anomaly*, *JHEP* **05** (2020) 061 [arXiv:1912.12956] [INSPIRE].

[44] KATRIN collaboration, *Bound on 3+1 Active-Sterile Neutrino Mixing from the First Four-Week Science Run of KATRIN*, *Phys. Rev. Lett.* **126** (2021) 091803 [arXiv:2011.05087] [INSPIRE].

[45] J. Kotila and F. Iachello, *Phase space factors for double-β decay*, *Phys. Rev. C* **85** (2012) 034316 [arXiv:1209.5722] [InSPIRE].

[46] D. Štefánik, R. Dvornický, F. Šimkovic and P. Vogel, *Reexamining the light neutrino exchange mechanism of the 0νββ decay with left- and right-handed leptonic and hadronic currents*, *Phys. Rev. C* **92** (2015) 055502 [arXiv:1506.07145] [InSPIRE].

[47] M. Horoi and A. Neacsu, *Towards an effective field theory approach to the neutrinoless double-beta decay*, arXiv:1706.05391 [InSPIRE].

[48] S. Stoica and M. Mirea, *New calculations for phase space factors involved in double-β decay*, *Phys. Rev. C* **88** (2013) 037303 [arXiv:1307.0290] [InSPIRE].

[49] A. Nicholson et al., *Heavy physics contributions to neutrinoless double beta decay from QCD*, *Phys. Rev. Lett.* **121** (2018) 172501 [arXiv:1805.02634] [InSPIRE].

[50] J. Engel and J. Menéndez, *Status and Future of Nuclear Matrix Elements for Neutrinoless Double-Beta Decay: A Review*, *Rept. Prog. Phys.* **80** (2017) 046301 [arXiv:1610.06548] [InSPIRE].

[51] J. Menéndez, *Neutrinoless ββ decay mediated by the exchange of light and heavy neutrinos: The role of nuclear structure correlations*, *J. Phys. G* **45** (2018) 014003 [arXiv:1804.02105] [InSPIRE].

[52] J. Hyvärinen and J. Suhonen, *Nuclear matrix elements for 0νββ decays with light or heavy Majorana-neutrino exchange*, *Phys. Rev. C* **91** (2015) 024613 [InSPIRE].

[53] EXO-200 collaboration, *Search for Neutrinoless Double-β Decay with the Complete EXO-200 Dataset*, *Phys. Rev. Lett.* **123** (2019) 161802 [arXiv:1906.02723] [InSPIRE].

[54] P.D. Bolton, F.F. Deppisch, L. Gráf and F. Šimkovic, *Two-Neutrino Double Beta Decay with Sterile Neutrinos*, *Phys. Rev. D* **103** (2021) 055019 [arXiv:2011.13387] [InSPIRE].

[55] M. Agostini, E. Bossio, A. Ibarra and X. Marcano, *Search for Light Exotic Fermions in Double-Beta Decays*, *Phys. Lett. B* **815** (2021) 136127 [arXiv:2012.09281] [InSPIRE].

[56] NEMO-3 collaboration, *Detailed studies of ^{100}Mo two-neutrino double beta decay in NEMO-3*, *Eur. Phys. J. C* **79** (2019) 440 [arXiv:1903.08084] [InSPIRE].

[57] J. Kopp, P.A.N. Machado, M. Maltoni and T. Schwetz, *Sterile Neutrino Oscillations: The Global Picture*, *JHEP* **05** (2013) 050 [arXiv:1303.3011] [InSPIRE].

[58] A. Falkowski, M. González-Alonso and Z. Tabrizi, *Reactor neutrino oscillations as constraints on Effective Field Theory*, *JHEP* **05** (2019) 173 [arXiv:1901.04553] [InSPIRE].

[59] I. Doršner, S. Fajfer, A. Greljo, J.F. Kamenik and N. Košnik, *Physics of leptoquarks in precision experiments and at particle colliders*, *Phys. Rept.* **641** (2016) 1 [arXiv:1603.04993] [InSPIRE].

[60] CMS collaboration, *Search for pair production of first-generation scalar leptoquarks at $\sqrt{s} = 13$ TeV*, *Phys. Rev. D* **99** (2019) 052002 [arXiv:1811.01197] [InSPIRE].

[61] ATLAS collaboration, *Search for pairs of scalar leptoquarks decaying into quarks and electrons or muons in $\sqrt{s} = 13$ TeV pp collisions with the ATLAS detector*, *JHEP* **10** (2020) 112 [arXiv:2006.05872] [InSPIRE].

[62] P.O. Ludl and W. Rodejohann, *Direct Neutrino Mass Experiments and Exotic Charged Current Interactions*, *JHEP* **06** (2016) 040 [arXiv:1603.08690] [InSPIRE].

[63] B. Grzadkowski, M. Iskrzyński, M. Misiak and J. Rosiek, *Dimension-Six Terms in the Standard Model Lagrangian*, *JHEP* **10** (2010) 085 [`arXiv:1008.4884`] [ɪɴSPIRE].

[64] Y. Liao and X.-D. Ma, *Operators up to Dimension Seven in Standard Model Effective Field Theory Extended with Sterile Neutrinos*, *Phys. Rev. D* **96** (2017) 015012 [`arXiv:1612.04527`] [ɪɴSPIRE].

[65] J. Barea, J. Kotila and F. Iachello, *Limits on sterile neutrino contributions to neutrinoless double beta decay*, *Phys. Rev. D* **92** (2015) 093001 [`arXiv:1509.01925`] [ɪɴSPIRE].

[66] J. Barea, J. Kotila and F. Iachello, *0νββ and 2νββ nuclear matrix elements in the interacting boson model with isospin restoration*, *Phys. Rev. C* **91** (2015) 034304 [`arXiv:1506.08530`] [ɪɴSPIRE].

[67] J. Barea, private communication.

[68] F.F. Deppisch, L. Gráf, F. Iachello and J. Kotila, *Analysis of light neutrino exchange and short-range mechanisms in 0νββ decay*, *Phys. Rev. D* **102** (2020) 095016 [`arXiv:2009.10119`] [ɪɴSPIRE].

[69] V. Cirigliano, W. Dekens, J. de Vries, M. Hoferichter and E. Mereghetti, *Toward Complete Leading-Order Predictions for Neutrinoless Double β Decay*, *Phys. Rev. Lett.* **126** (2021) 172002 [`arXiv:2012.11602`] [ɪɴSPIRE].

[70] V. Cirigliano, W. Dekens, J. de Vries, M. Hoferichter and E. Mereghetti, *Determining the leading-order contact term in neutrinoless double β decay*, *JHEP* **05** (2021) 289 [`arXiv:2102.03371`] [ɪɴSPIRE].